

Age and composition of final stage of volcanism in Okhotsk-Chukotka volcanic belt: An example from the Ola Plateau (Okhotsk Segment)

V. V. Akinin¹, P. Layer², J. Benowitz², Ntaflos, Th.³

¹North-East Interdisciplinary Scientific Research Institute, FEB Russian Academy of Science, Magadan, 685000, Russian Federation

²University of Alaska, Fairbanks, AK 99775, USA

³Department of Lithospheric Research, University of Vienna, Austria

ABSTRACT

The final stage of volcanism in the subduction-related Okhotsk-Chukotka volcanic belt (OCVB) is represented by transitional basalts and andesitic basalt lava flows of the Mygdykit unit forming several separated high-altitude plateaus. One of the largest is the Ola plateau (~222 km³), which is located north of the Okhotsk Sea and yields Early Campanian (~78–80 Ma) ⁴⁰Ar/³⁹Ar and U-Pb ages. The Ola plateau basalts formed less than 2 Ma after the eruption of underlying rhyolite sequences of the main phase of the OCVB and therefore are regarded as part of OCVB. The new ages date the cessation of volcanism and time of the change in the locus of arc volcanism to more eastern locations along the margin of the paleo-Pacific ocean in the Maastrichtian and Paleocene (i.e., the Bristol-Anadyr and Koryak-Kamchatka arcs). This end of magmatism in the OCVB coincides with the timing of the final plume-related intraplate volcanism of the High Arctic Large Igneous Province (HALIP). Although the Ola plateau basalts have some subduction-related geochemical features (e.g. Nb-Ta negative anomaly) they also display geochemical discrepancies compared to basalt units in the older part of the OCVB, such as the higher contents of Ti, Zr, P, and other high field strength elements as well as more evolved Sr, Nd isotopic ratios. The origin of the late-stage basaltic magmas of the OCVB are attributed to weak assimilation and fractional crystallization processes in deep magma chambers during an interval of local extension due to the change in geodynamic setting from frontal subduction to a slab-window transform regime along the paleomargin of eastern Asia.

INTRODUCTION

One of the key problems in continental margin geology is the mechanism responsible for cessation of subduction and coeval magmatism in a continental margin arc. The cause of the demise of the arc might be reflected in changes in the chemistry of the final volcanism events which emphasizes the importance of compositional studies on such late-stage arc magmas. Another topic related to the importance of precise characterization of early and late-stage volcanism particularly in the case of two attached and/or overlaid arcs is to be able to distinguish them. Such issues have been debated for a long time for the continental margin of northeastern Russia where Okhotsk-Chukotka volcanic belt (OCVB) sits on older arcs and is, in turn, overlain by the slightly younger Bristol-Anadyr and Koryack-Kamchatka volcanic belts (e.g. Bely, 1977; Filatova, 1988; Kotlyar and Rusakova, 2004; Akinin and Miller, 2011). Hourigan and Akinin (2004) dated the final stage of volcanism in the Arman plateau using the ⁴⁰Ar/³⁹Ar method but there are other regional plateau basalts of unknown age that need to be investigated. Do they have the same age or do they show some spatial-temporal progression? For instance, Stone et al. (2009) reported about 10 Ma younger ⁴⁰Ar/³⁹Ar ages for upper basalts in Enmyvaam volcanic field of OCVB compared to Hourigan and Akinin (2004) results from the area. Additionally, compositions of these late-stage basalts are poorly studied, particularly in terms of modern trace element and isotopic geochemistry which is critical to understanding the tectonic setting and evolution of the final stages of the OCVB.

There are some fundamental topics that could also potentially be addressed if the mechanism of arc demise can be identified. Change in direction of

oceanic plate motion is one of the possible tectonic scenarios leading to subduction cessation (e.g. Matthews et al., 2012). Why do some subduction zones roll back along the trench and how fast does this process occur are still open questions. Driving mechanisms of plate reorganizations responsible for major episodes of plate motion change remain unclear (e.g. Bercovici, 2003), including the importance of top-down (plate-derived) (Anderson, 2001) versus bottom-up (mantle flow-derived) (e.g. King et al., 2002) processes. There are asymmetries on both sides of Tethys (paleo Pacific) Ocean margins in terms of occurrences of modern island arcs and back arc basins which can be related to different

angles of oceanic and continental plates interaction (frontal subduction in western Pacific vs. transform slip in north-eastern Pacific) (Seton et al., 2012). Are there any correlations in age and composition of arc magmatism on both sides of Pacific? The OCVB (Fig. 1) stretching about 3250 km along the margin of North Asian continent, from the mouth of the Uda River in the Khabarovsk District to Provideniya on the eastern Chukchi Peninsula is the perfect location to investigate both these regional and general process questions.

The OCVB comprises about 1 million km³ of Cretaceous calc-alkaline volcanic rock suites consisting of andesitic basalts, andesites, dacites,

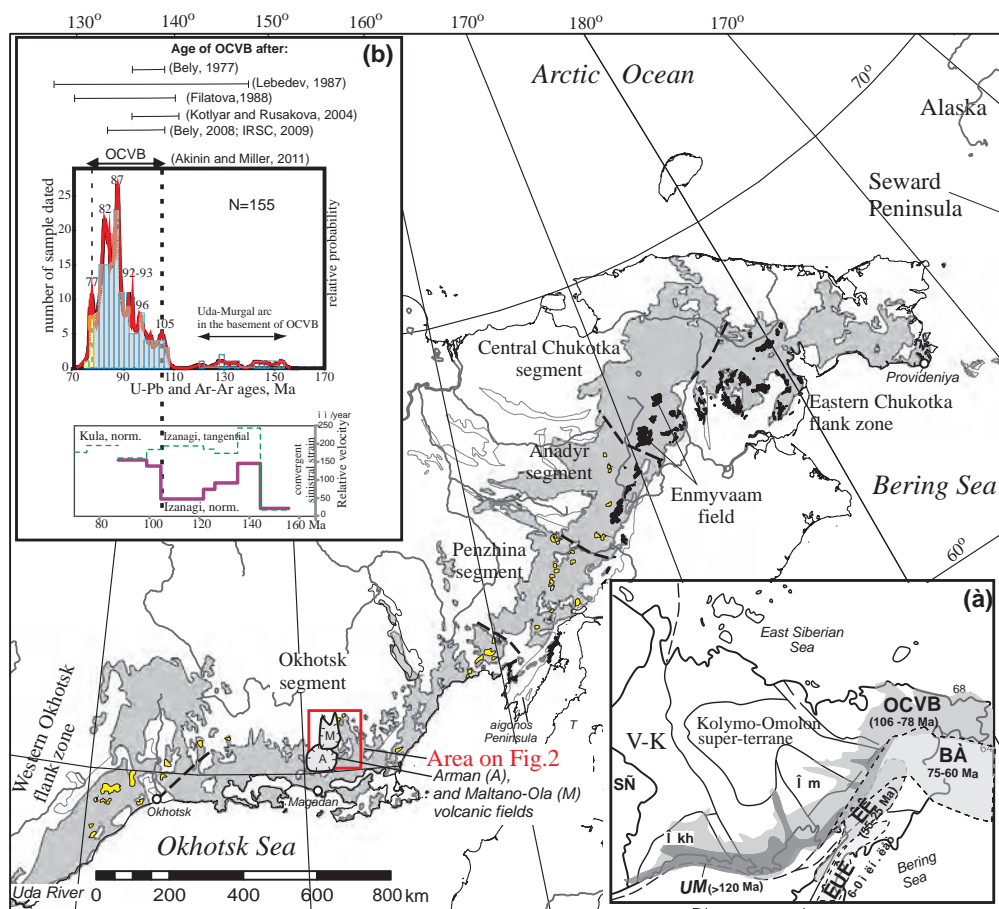


Fig. 1. Sketch map showing the Okhotsk –Chukotka volcanic belt in the continental framework of northeastern Asia (after Akinin and Miller, 2011; with minor changes). The names of the main segments and flank zones of the belt are after Belyi (1977). Gray shading shows the main volume of the Albian – Campanian calc-alkaline magmas of the OCVB, yellow areas are exposures of the Campanian late OCVB plateau basalts, and oblique hatching shows pre-OCVB island-arc volcanosedimentary complexes. Black areas are Maastrichtian-Paleocene basalts of Bristol-Anadyr and Koryak-Kamchatka belts which are located east of the OCVB. Inserts: (a) distribution of volcanogenic belts in northeastern Asia showing a decrease in age toward the paleo-Pacific (UM, Uda–Murgal; OCVB, Okhotsk–Chukotka; BA, Bristol–Anadyr; KK, Koryak–Kamchatka; and KUK, Kuril–Kamchatka). Lines show the boundaries of main terranes, and cross-hatching pattern shows Precambrian cratons and microcontinents that underlie the volcanic belts. Abbreviations: SC, Siberian craton; Okh, Okhotsk massif; and Om, Omolon massif. (b) Histogram of the U-Pb and ⁴⁰Ar/³⁹Ar ages of igneous rocks in OCVB and Uda-Murgal arc showing the correspondance of the volcanism with the changing direction and rate of movement of Pacific oceanic plates during the Cretaceous (Akinin and Miller, 2011).

rhyolites, their tuffs and tuffaceous sediments as well as coeval magnetite-bearing granitoid intrusions. The OCVB is a classical Andean-style arc but differs in some details because it was built on thinner (around ~30 to ~35 km) and variable age crust (Archean to Paleoproterozoic basement is seen in the Okhotsk and Omolon microcontinents, while Paleozoic to Early Cretaceous forms the remainder of the regional basement). All volcanic deposits of the main-stage of the OCVB are typical calc-alkaline rocks showing considerable variations in alkalinity and relatively high SiO₂ contents at low Fe/Mg. The OCVB arc is interpreted as having formed from subduction of part of the ancestral Pacific oceanic plate during the Albian to Campanian. Forearc basins are preserved in the West Kamchatka, Ekonay, and Yanranay accretionary-wedge terranes (Parfenov, 1984). One of the key aspects of the OCVB is that the belt overlaps terranes of both the Pacific and Arctic continental margins, constraining and linking their tectonic evolution.

The age span of the OCVB is still a topic of debate. It was first estimated as Neocomian–Paleogene (Ustiev, 1959; Umitbaev, 1986), then Albian–Cenomanian (Belyi, 1977; Kotlyar and Rusakova, 2004; Zhulanova et al., 2007), then Albian–Paleogene (Filatova, 1988), and then middle Albian–Santonian (Belyi, 2008; Koren' and Kotlyar, 2009). The lack of consensus is related to the original geochronological methods used (paleophytological methods and bulk rock K–Ar and Rb–Sr isotope analysis) which produced variable and non reproducible ages.

The first ⁴⁰Ar/³⁹Ar and U–Pb mineral ages from the volcanic rocks of the OCVB provided new insight into the inception, total duration, and variations in style and age of volcanism in the different segments of the belt (Kelley et al., 1999; Newberry et al., 2000; Hourigan and Akinin, 2004; Ispolatov et al., 2004; Akinin and Miller, 2011; Tikhomirov et al., 2012). The geochronologic results are fundamentally different from previously accepted ages of the OCVB and require a revision of the existing chronostratigraphic and tectonic models of the OCVB development which will continue to benefit from additional investigations using modern isotopic methods.

The volcanic rocks of the OCVB are flat-

lying, undeformed, and overlap the previously accreted Kolyma-Omolon superterrane and adjacent collisional belts in the Russian Northeast. Knowledge of the temporal evolution of the OCVB is critical for understanding the final timing of accretion of those terranes as well as the upper age limit of accretion tectonics in the region. The economic implications of any OCVB investigation are great because the belt hosts many epithermal gold-silver deposits of low sulfidation types (more than 50 epithermal deposits have been explored in northeastern Asia, from which more than 150 metric tons of gold and more than 1000 metric tons of silver have been recovered during the past 70 years; Struzhkov and Konstantinov, 2005). Of particular importance to economic development is having knowledge of the precise age of the final stage of basaltic volcanism in OCVB. Basaltic dikes mapped in many epithermal ore deposits post-date all of the units including gold-bearing quartz-adularia veins thus constraining the upper limit age of the mineralization.

The final stage of volcanism in the OCVB is represented by local basaltic plateaus (Fig. 1, yellow). One of the most renowned OCVB researchers, V.F. Belyi (Belyi, 1977; Belyi, 2008), argued that these late stage basaltic lavas should be included as part of the OCVB, although others have disagreed, pointing out discrepancies in their geochemical signatures, ages and geodynamic settings ((Filatova, 1988; Polin and Moll-Stalcup, 1998; Kotlyar and Rusakova, 2004). In our opinion, the discrepancies apply mainly to basalts in the northeastern part of the OCVB (Enmyvaam volcanic field, and Amguema–Kanchalan volcanic field (Stone et al., 2009; Sakhno et al., 2010) where ~60 to ~67 Ma-old (Maastrichtian to Paleocene) basalts overlap the OCVB and display a ~10 Ma hiatus after eruption of upper OCVB rhyolites. By this reasoning, we argue that Maastrichtian and younger volcanic rocks belong to the younger Bristol-Anadyr and Koryak-Kamchatka volcanic belts which are located east of the OCVB (Akinin et al., 2009; Akinin and Miller, 2011). If, on the other hand, hiatuses are short (within the uncertainty of age determination, ~1–~2 Ma) between arc volcano-sedimentary sequences that directly adjoin or occur in nearby areas, then it is likely that they constitute part of the same arc volcanic sequence.

In this paper we present geochronologic evidence that the Ola basaltic plateau formed between ~78 to ~80 Ma using $^{40}\text{Ar}/^{39}\text{Ar}$ and U-Pb SHRIMP dating. These ages are close to those from the underlying rhyolite sequences with the gap between the two volcanic units being no longer than 1–2 Ma. The short span of time separating the two volcanic units gives us reason to consider the plateau basalts to be part of the OCVB. Systematic weak upward compositional changes in the basaltic unit are interpreted as being related to limited fractional crystallization combined with assimilation and following alteration. The final stage of basaltic volcanism in the OCVB (ca. 78-79 Ma) reflected changes in geodynamic setting from subduction to

transform slip and closely corresponds in age to the final stage of High Arctic Large Igneous Province (HALIP) volcanism of the Arctic region (Gottlieb and Miller, 2012).

GEOLOGIC SETTING AND PREVIOUS WORK

Located along the northern shore of the Okhotsk Sea (from the town of Okhotsk to the Taigonos Peninsula), the OCVB is subdivided into segments or “sectors” on the basis of differences in the basement rock types and lithologic similarities of volcanic rocks within specific geographic regions (Bely, 1977). A typical cross-section of the OCVB in the Okhotsk segment can be seen in the Arman and

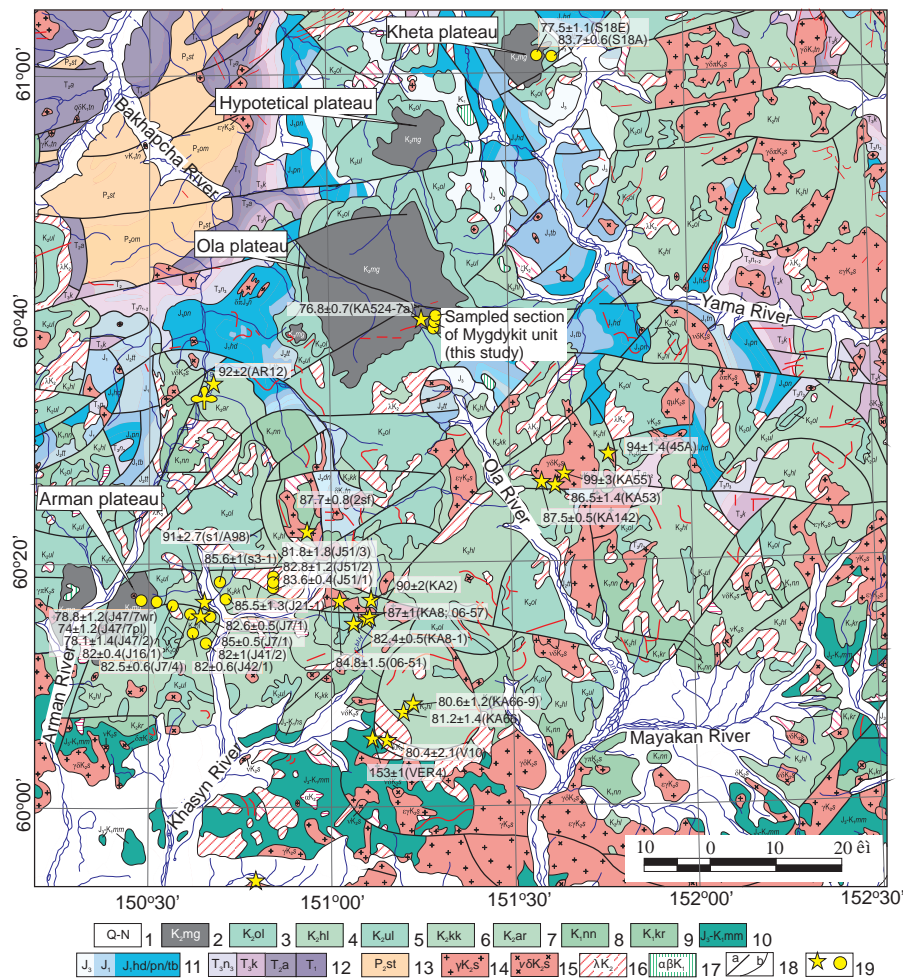


Fig. 2. Geological map of southern part of the Okhotsk segment of the Okhotsk-Chukotka volcanic belt (compiled using Gorodinsky, 1980). 1–Quaternary alluvium and lake deposits, 2–9–volcanic units of OCVB (2–Mygdykit, 3–Ola, 4–Kholchan, 5–Ulyn, 6–Kukushka or Narauli, 7–Arman, 8–Nankala, 9–Kirik, 10–Momoltykich unit of Uda-Murgal arc in the base of OCVB, 11–Jurassic sediments, 12–Triassic sediments; 13–Permian sediments, diamictites and phillites; 14–15–Upper Cretaceous granite (14), and gabbro-diorite (15) intrusions. 16–17–Upper Cretaceous subvolcanic intrusions of rhyolites (16), and basaltic andesites (17). 18–faults (a) and contacts (b). 19– samples dated by U-Pb SHRIMP (stars - Akinin and Miller, 2011) and $^{40}\text{Ar}/^{39}\text{Ar}$ (circle - Hourigan and Akinin, 2004) methods, dates and uncertainty shown in Ma, sample number in brackets.

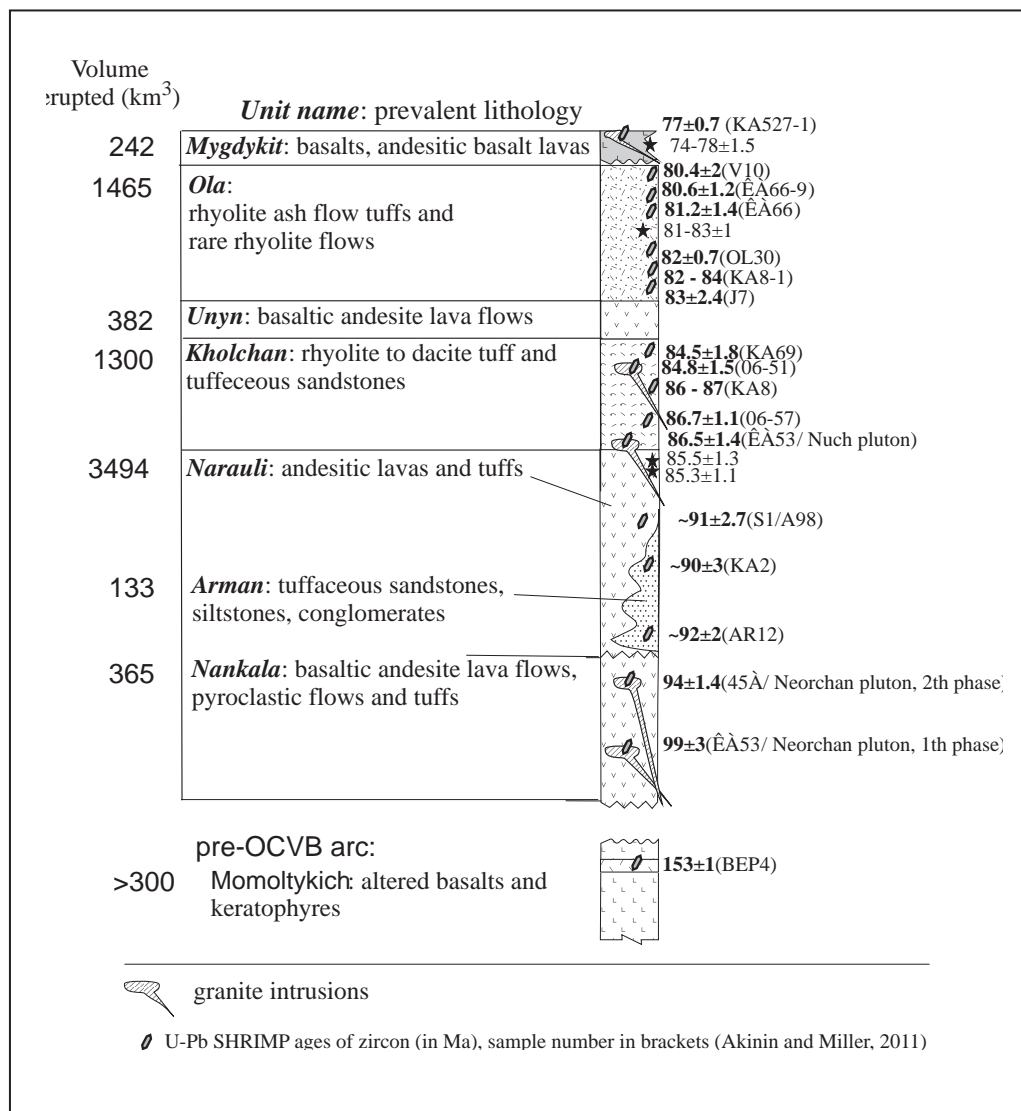


Fig. 3. Generalized stratigraphic column of volcanic units in Arman and Maltano-Ola volcanic fields (Okhotsk segment of OCVB). Volcanic units are according to (Anorov et al., 1999), volcanic volume erupted and isotopic ages are after Akinin and Miller (2011).

Maltano-Ola volcanic fields (fields called structures in Russian literature) (Figs. 1 and 2). Those two volcanic fields delineate a ~1500 km² area, where the total thickness of the volcanic sequences is 1–2 km and the thickness of each volcanic unit is highly variable. A simplified succession in the area is presented in Fig. 3.

All of the main stage volcanic products (Nankala to Ola units on Fig. 3) are typical calc alkaline rocks showing considerable variation in alkalinity and relatively high SiO₂ contents at low Fe/Mg. Late-stage basaltic volcanism of the Mygdykit unit forms several distinctive plateaus including the Yana, Arman, Kheta, Hypotetical and Ola (grey fields on Fig. 2). One can integrate Ola and Mygdykit units

into bimodal formation, but Hourigan and Akinin (2004) reported a ~3 Ma hiatus between those two units precluding bimodal origin from the single same source. They follow the conclusions of previous studies (Filatova, 1988; Polin and Moll-Stalcup, 1999) which point toward a within-plate, possibly extension-related origin of late-stage basalts of the Arman plateau, but this conclusion needs to be proved or disproved using detail geochemical and geochronological study of the different plateaus.

The Ola plateau is one of the largest, and is composed of Mygdykit unit basalts. It is also well known because of gem deposits of agates and chalcidonites associated with the basalts. The Ola plateau is located in the headwaters of Ola River,

Magadan district (north of the Okhotsk Sea) and is recognized by a planar primary surface that dips gently to the northwest at an elevation of ~1500 m (Figs. 3 and 4). Basalts of the Mygdykit unit on the Ola plateau occupy ~443 km² and have an estimated total eruptive volume of ~222 km³ (assuming an average ~500 m thickness; Akinin et al., 2007). The age of the Mygdykit basalt unit was thought to be Cenomanian (Belyi, 1977) or Maastrichtian to Paleogene (Filatova, 1988) based on early work using paleo-flora assemblages. The age of the basalts was later changed to Santonian and probably Early Campanian based on palynocomplexes and a few whole rock K-Ar and ⁴⁰Ar/³⁹Ar ages (Belyi and Belaya, 1998). Filatova (1988) first suggested that Maastrichtian-Paleocene plateau basalts located within the OCVB region and in the inner zones of Koryak-Kamchatka region are not related to subduction-related OCVB volcanism, but rather are extensional basalts deposited in local grabens formed in response to Late Cretaceous and Paleogene collision of oceanic island arcs against the Russian Far East. Alshevsky (1997) reported the first K-Ar whole-rock ages for the Ola, Kheta, and

Arman plateau basalts ranging from 81 ± 1 Ma to 63 ± 3 Ma, and concluded a Paleocene age for the upper age limit of the OCVB. Kotlyar and Rusakova (2004) suggested a Santonian – Early Campanian age (84 – 82 Ma) for the upper plateau basalts by picking a “true relict age” using only the oldest published K-Ar whole rock data. They ignored the few existing ⁴⁰Ar/³⁹Ar ages at the time and included the upper basalts of the “Khakarino-Enmyvaam intercontinental volcanic chain” which post-dates the OCVB (Kotlyar and Rusakova, 2004; Zhulanova et al., 2007) basically following the conclusions of Filatova (1988). The rhyolites of Ola units which concordantly underlie the lower basaltic flows of the Mygdykit unit, yielded ~83 to ~81 Ma ⁴⁰Ar/³⁹Ar ages (Hourigan and Akinin, 2004; Akinin and Miller, 2011). Thus the age of the Mygdykit unit has been debated for decades and needs to be resolved using modern geochemical and isotopic geochronology methods such as ⁴⁰Ar/³⁹Ar and U-Pb on other regional basalt plateaus.

This study focuses on the Ola basaltic plateau on the right bank of Grozovoi Creek where 97 individual lava flows with a total thickness of ~630 m

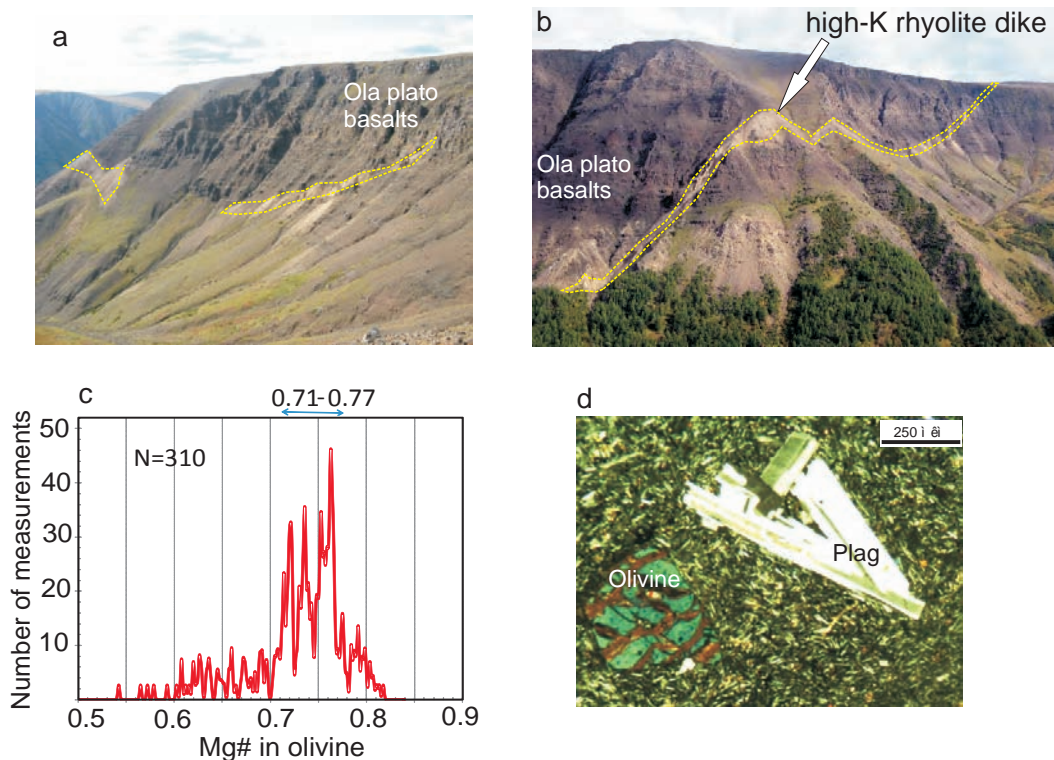


Fig. 4. Mygdykit unit basalts in Ola plateau . Yellow line in the 4a and 4b photo shows the high-potassium rhyolite dike cutting the basaltic section. 4c – Distribution of olivine phenocrysts composition (Mg# = Mg/ (Mg+Fe), molar fraction). 4d – typical thin-section of Mygdykit unit basalts.

are recognized (Fig. 4). Each lava flow is 3 to 6 m thick and is composed of brecciated reddish basaltic clastic lava at the base, massive lava in the middle, and vesicular lavas at the top of each flow. Massive lava from the middle part of each flow was sampled and numbered sequentially from B1 to B97, and then samples were submitted for major and trace element geochemistry. In addition, several key samples were dated using the $^{40}\text{Ar}/^{39}\text{Ar}$ method and the composition phenocryst phases determined by microprobe analysis. The basalt flows are cut by a high-potassium rhyolite dike which provides a good constraint on upper age limit for the Mygdykit basalts on the Ola plateau.

ANALYTICAL METHODS

The samples were studied in thin-sections using classical microscopy for petrographic analysis. Mineral compositions were measured on a Camebax microprobe (NEISRI, Far East Branch, Russian Academy of Science, Magadan) and a JEOL microprobe (Vienna University, Austria), using common measurements conditions (15kV, 20nA), and a set of synthetic and natural standards. ZAF corrections were applied for matrix effects. Uncertainties of measurements were less than 5% (excluding Na). X-ray fluorescence analysis of whole rocks for major and trace elements were performed at NEISRI (Far East Branch, Russian Academy of Science, Magadan) using SRM-25 and VRA-30 spectrometers and following standard procedures. Uncertainties for major element abundances were less than 0.4% for SiO_2 and about 0.2% for other oxides; errors for trace element measurements (Rb, Sr, Zr) did not exceed 5–6%. ICP-MS analyses for trace elements were performed at the Institute of Tectonics and Geophysics (Far East Branch, Russian Academy of Science, Khabarovsk) and IEC SB RAS (Irkutsk) where repeated measurement of BHVO-1, AGV-1 and BIR-1 standards yielded a 5 to 10% standard deviation. The distribution of major and trace elements allow us to estimate the role of crystal fractionation and magma mixing in the petrogenesis of the OCVB volcanic rocks and to perform geochemical modeling using available computer software programs. Melt crystallization was simulated using COMAGMAT software (Ariskin and Barmina, 2000), and mineral thermobarometry

was carried out using olivine-melt and plagioclase-melt thermobarometers (Putirka, 2008). The mass spectrometric measurements of Sr, Nd, and Pb isotopic ratios in the bulk rocks of the OCVB were carried out using a MI-1201 mass spectrometer at NEISRI (Magadan) and a VG-Sector mass spectrometer (Stanford University, United States).

For $^{40}\text{Ar}/^{39}\text{Ar}$ analysis, samples were submitted to the Geochronology Laboratory at University of Alaska Fairbanks where they were crushed, sieved, washed and hand-picked for small phenocryst-free whole-rock chips. The mineral standard MMhb-1 (Samson and Alexander, 1987) with an age of 513.9 Ma (Lanphere and Dalrymple, 2000) was used to monitor neutron flux (and calculate the irradiation parameter, J). The samples and standards were wrapped in aluminum foil and loaded into aluminum capsules of 2.5 cm diameter and 6 cm height. The samples were irradiated in position 5c of the uranium enriched research reactor of McMaster University in Hamilton, Ontario, Canada for 20 megawatt-hours.

Upon return from the reactor, the samples and monitors were loaded into 2 mm diameter holes in a copper tray that was then loaded into an ultra-high vacuum extraction line. The monitors were fused and samples heated using a 6-watt argon-ion laser following the technique described by York et al. (1981), Layer et al. (1987) and Layer (2000). Argon purification was achieved using a liquid nitrogen cold trap and a SAES Zr-Al getter at 400C. The samples were analyzed in a VG-3600 mass spectrometer. The measurements of argon isotopes were corrected for system blank and mass discrimination, as well as calcium, potassium and chlorine interference reactions following procedures outlined in McDougall and Harrison (1999). System blanks generally were 2×10^{-16} mol ^{40}Ar and 2×10^{-18} mol ^{36}Ar which are 10 to 50 times smaller than the values for the fraction volumes. Mass discrimination was monitored by running both calibrated air shots and a zero-age glass sample. These measurements were made on a weekly to monthly basis to check for changes in mass discrimination.

A summary of all the $^{40}\text{Ar}/^{39}\text{Ar}$ results is given in Table 1, with all ages quoted to the ± 1 sigma level and calculated using the constants of Steiger and Jaeger (1977). The integrated age is the age given by the total gas measured. The spectrum provides a

plateau age if three or more consecutive gas fractions represent at least 50% of the total gas release and are within two standard deviations of each other (Mean Square Weighted Deviation less than 2.5). Each sample was run twice to both confirm age determinations and to optimize analytical precision.

RESULTS

⁴⁰Ar/³⁹Ar age of Mygdykit unit of Ola plateau

Six whole rock samples were dated using the ⁴⁰Ar/³⁹Ar method. Five samples (B2 to B7) are from the bottom of the “B” cross-section, and one sample (B91) was collected from the top of section. The ⁴⁰Ar/³⁹Ar data suggest that the emplacement of the entire section of Mygdykit unit in Ola plateau occurred between 80.6 ± 1.2 to 76.6 ± 0.7 Ma (weighted mean = 78.6 ± 1.9 [2.5%] 95% conf., MSWD = 4.3, probability = 0.001). The results

of five of the samples (B2, B3, B5, B7, and B91) are consistent and are in agreement with their stratigraphic positions in the succession (Table 1). There is a very high probability that entire section of basalts erupted almost synchronously bearing in mind the overlap of uncertainty obtained between about 78 and 79 Ma. The only exception to this interpretation is sample B4 which yielded an older plateau and inverse isochron ages of 82.0 ± 1.1 Ma (Table 1), but this age is still within two sigma error of the weighted mean age of the other four samples. The upper limit of Mygdykit unit formation can be constrained by the age of a rhyolite dike which cuts the basalt section (Fig. 5). Zircon from a dike of peralkaline rhyolites cutting the Mygdykit basalts in Ola Plateau were dated previously using SHRIMP-RG (Akinin and Miller, 2011) and yielded a mean weighted age of 76.8 ± 0.7 Ma

Table 1. Summary of ⁴⁰Ar/³⁹Ar geochronological data.

Sample	Min.	Integrated Age (Ma)	Plateau Age (Ma)	Plateau Information	Isochron Age (Ma)	Isochron Information
B2	WR	89.0± 3.3	80.6± 1.2	8 of 11 fractions 62.9% ³⁹ Ar release MSWD =0.6	79.0 ± 1.2	8 of 12 fractions ⁴⁰ Ar/ ³⁶ Ari = 304.5 ± 3.1 MSWD = 0.6
B3	WR	80.6± 1.1	78.6± 0.8	9 of 11 fractions 82.7 % ³⁹ Ar release MSWD =1.1	77.9 ± 0.9	12 of 12 fractions ⁴⁰ Ar/ ³⁶ Ari = 300.0 ± 2.0 MSWD = 1.0
B4	WR	84.5± 1.5	82.1± 1.1	7 of 12 fractions 81.1 % ³⁹ Ar release MSWD =0.6	82.0 ± 1.1	12 of 12 fractions ⁴⁰ Ar/ ³⁶ Ari = 302.8 ± 3.1 MSWD = 0.6
B5	WR	79.2± 2.2	79.3± 1.4	5 of 8 fractions 72.2 % ³⁹ Ar release MSWD =0.2	79.3.0 ± 1.4	8 of 8 fractions ⁴⁰ Ar/ ³⁶ Ari = 294.8 ± 4.2 MSWD = 0.2
B7	WR	81.2± 1.2	78.2± 0.7	4 of 9 fractions 77.2 % ³⁹ Ar release MSWD =0.1	78.0± 0.9	7 of 9 fractions ⁴⁰ Ar/ ³⁶ Ari = 298.8 ± 4.7 MSWD = 0.3
B91	WR	77.5 ± 0.5	76.6 ± 0.7	3 of 7 fractions 56% ³⁹ Ar release MSWD = 2.0	-	-

Samples analyzed with standard MMhb-1 an age of 513.9 Ma. A homogenous whole rock ground mass separate from each sample was analyzed. We prefer the plateau age (in bold) because of the higher precision, convention and because of the high atmospheric content of the first two to three steps and low K content of the final steps release. For geochemical data, see Table 2.

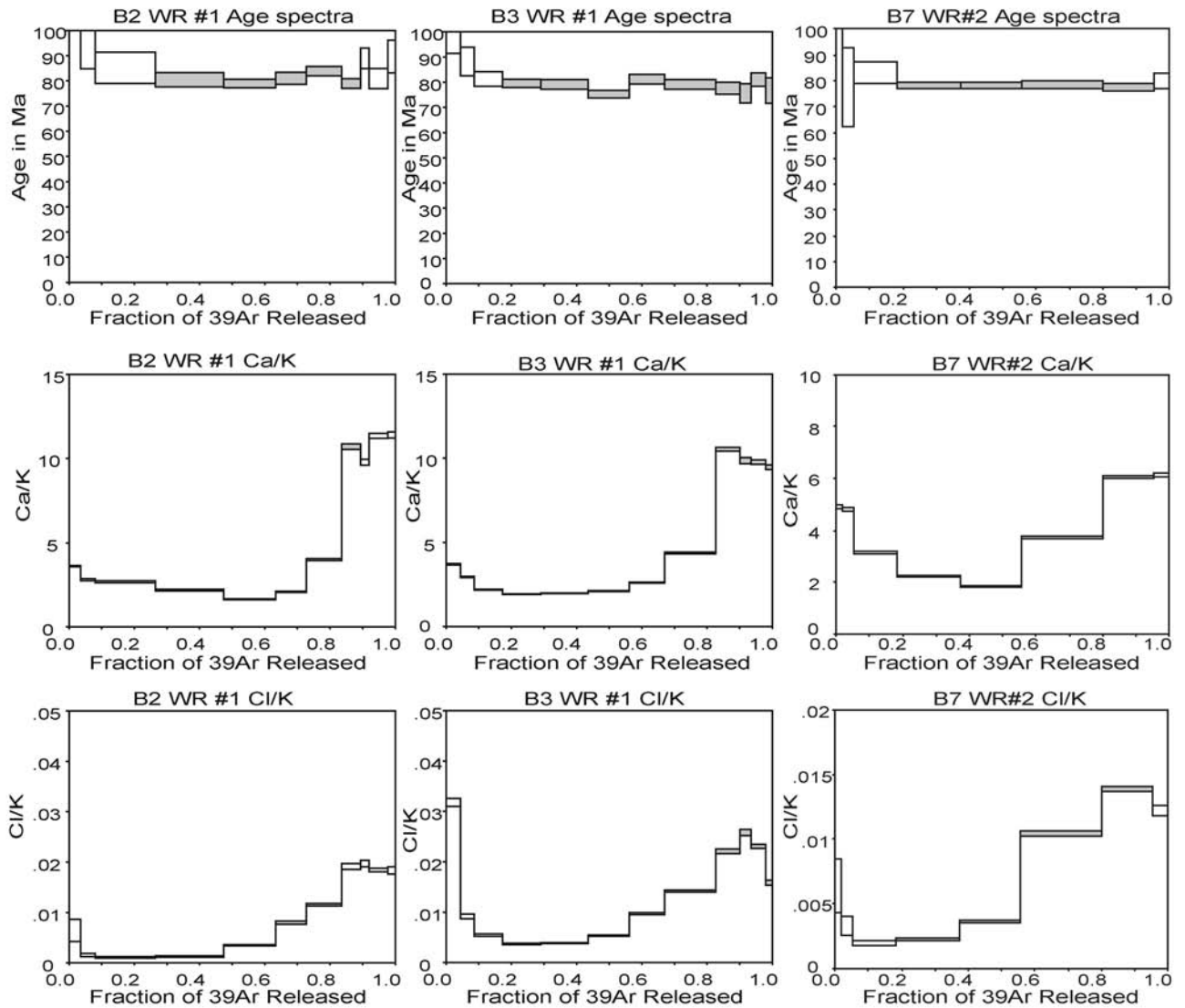


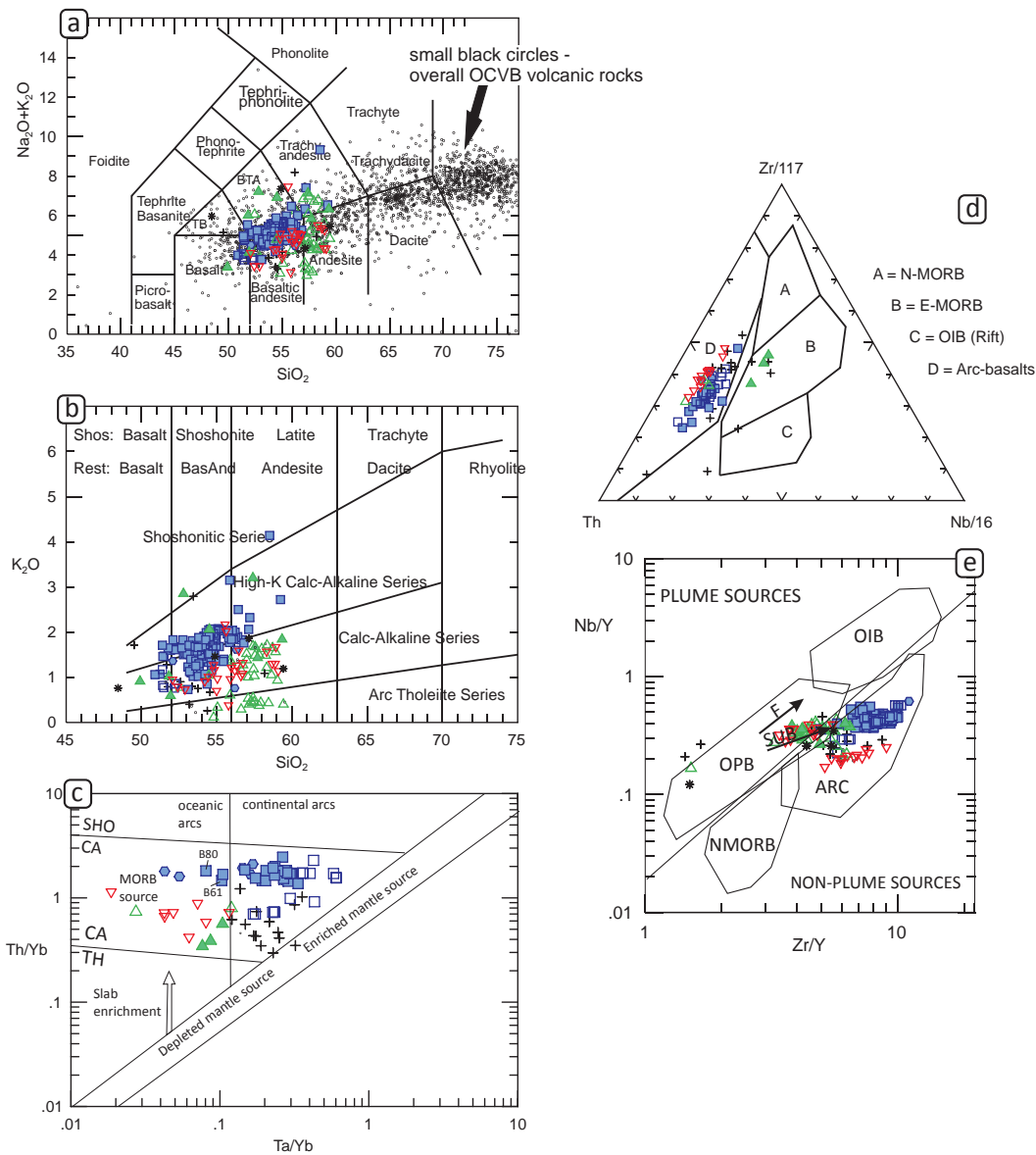
Fig. 5. Age spectrum, Ca/K, and Cl/K plots for three new $^{40}\text{Ar}/^{39}\text{Ar}$ analyses of Mygdykit unit basalts from Ola plateau. Sample localities are shown in Fig. 2.

(MSWD = 1.2, $N = 8/10$). The age of the rhyolite dike is consistent with our $^{40}\text{Ar}/^{39}\text{Ar}$ age on sample B91 and suggests a possible bimodal generation of basalts and rhyolite dikes. Previously published $^{40}\text{Ar}/^{39}\text{Ar}$ ages from the Mygdykit basalts from the Arman plateau located to the south-west from the Ola plateau yield ~ 74 to $\sim 77.5 \pm 1$ Ma ages demonstrating a quite prolonged eruption history (Hourigan and Akinin, 2004). Our new isotopic geochronologic data sets viewed as an entirety, provides an opposing view suggesting that the whole basalt section of Mygdykit unit may have been catastrophic and basalt generation occurred almost synchronously as essentially one eruptive phase, probably over a period of less than 1 Ma. The apparent difference in the two data sets loses significance if we exclude

just one sample from Hourigan and Akinin's (2004) data. The accepted 74 ± 1.2 Ma $^{40}\text{Ar}/^{39}\text{Ar}$ age for this "anomalous" sample (J47/7 plagioclase in Table 7, Hourigan and Akinin, 2004) is an isochron age which was not reproduced by an Ar-plateau age. In addition, a whole rock argon age for this sample yields an age of 78.8 ± 1.2 Ma which is 4.8 Ma older compared to its plagioclase age (J47/7 WRB in Table 7 of Hourigan and Akinin, 2004).

Variation of lava composition

Most of the studied lavas are unaltered and consist of olivine- and olivine-plagioclase porphyritic basalts and basaltic andesites (both referred to as basalts). Geochemical analyses shows that these rocks belong to normal to transitional



Basaltic to andesitic volcanic rocks of OCVB (Okhotsk segment), SiO₂ < 60 wt% in dry mode:

- top of OCVB section
 - Mygdykit unit Ola plateau ~ 78-79 Ma.
 - Mygdykit unit Hypotetical plateau ~ 76-78 Ma.
 - Mygdykit unit Arman plateau ~ 74-78 Ma (Horigan and Akinin, 2004).
- bottom of OCVB section
 - ▼ Ulyn unit ~ 85-83 Ma
 - ▲ Narauli unit ~ 85-90 Ma
 - ▲ Nankala unit ~ 100 Ma
- pre-OCVB volcanic rocks
 - + Momoltyk unit ~140-150 Ma
 - * Arman unit (pebble in conglomerate)

Fig. 6. Classification and discrimination geochemical diagrams for volcanic rocks of Okhotsk segment of OCVB located in the area outlined on Fig. 2. Mygdykit unit basaltic andesites have Arc-type signatures although they are enriched in potassium, Zr, and Ti compared to the rocks of basaltic and basaltic andesite composition from lower units of OCVB. (a, b) TAS classification diagram of LeBas et al. (1986) showing predominant basaltic andesite composition of Mygdykit unit volcanic rocks; (b) Arc rock types diagram of Peccerillo and Taylor (1976) showing trend to high-K calc-alkaline series for Mygdykit unit volcanic rocks compared to those from lower units of OCVB. (c) Ta/Yb vs. Th/Yb diagram after Pearce (1983), showing continental arc origin of Mygdykit unit basalts with enriched source of magma. SHO - shoshonitic series, CA - calc-alkaline series, TH - tholeiitic series. (d) Th-Zr-Nb diagram of Wood (1980) showing arc origin of Mygdykit unit basalts. (e) Zr/Y vs. Nd/Y diagram from (Condie, 2003) where arrows indicate effects of batch melting (F) and subduction (SUB). Abbreviations: ARC, arc-related basalts; NMORB, normal ocean ridge basalt; OIB, oceanic island basalt; OPB – oceanic plateau basalts (Pearce and Cann, 1973).

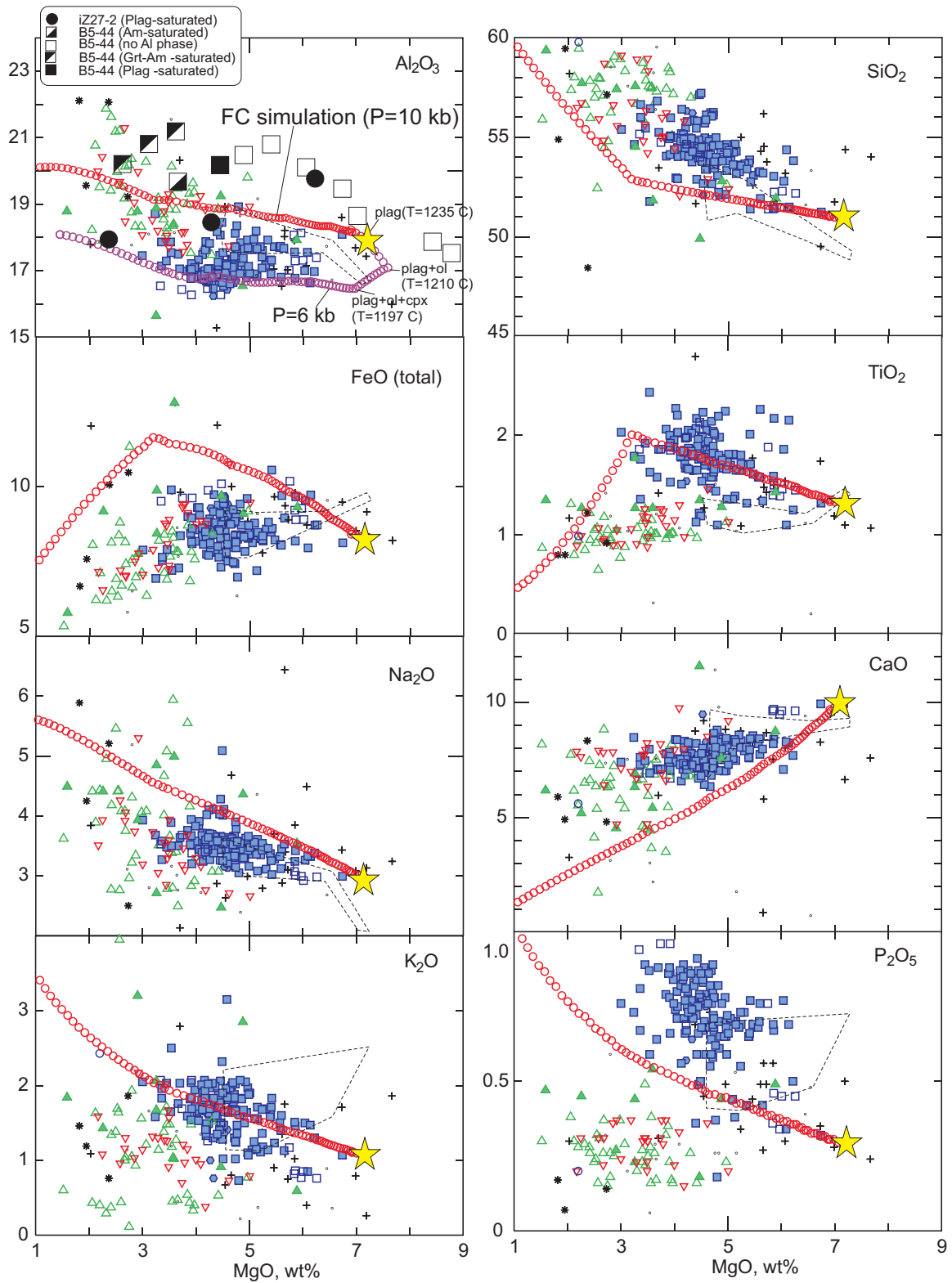


Fig. 7. Harker-type diagram for volcanic rocks of Okhotsk segment of OCVB. Red circle shows modeled fractional crystallization liquid line of descent (FC) simulated using COMAGMAT software (Ariskin and Barmina, 2000). Color symbols are OCVB samples as in Figure 6. Dashed line delineated field of basalts from Enmyvaam unit, Chukotka (Belyi and Belaya, 1998; Stone et al., 2009) which represent Maastrichtian volcanism of Bristol-Anadyr belt located east from OCVB. Black squares on SiO vs. Al_2O_3 diagram denote experimentally produced residual melts from crystallization of hydrous basalts in the lower crust. Primitive Mount Shasta basaltic andesite, sample 85-44 (mg-number 0.71), from Grove et al. (2003), at 0.8–1.2 GPa, 1045–1230° C and with >2.5 wt % added H_2O ; filled black circles denote experimental melts from Kawamoto (1996) on a Higushi-Izu high alumina basalt, sample IZ27-2 (mg-number 0.60), at 1.0 GPa, 1000–1150° C with 1 wt % added H_2O .

calc-alkaline series, and moderate to high alumina type (Figs. 6 and 7). Basalts of the Mygdykit unit are distinguished from basalts of lower units (such as Ulyn, Narauli, Nankala, and Momolykich units) because of higher contents of Ti, Zr, and rare earth elements (REE) and display some enriched intraplate-like geochemical signatures (Filatova, 1988; Polin and Moll-Stalcup, 1999; Akinin and Miller, 2011; Fig. 7). Nevertheless, Mygdykit unit basalts have a pronounced Nb-Ta negative trough on the spider diagram; a similar pattern to that as seen in the older subduction related volcanics of OCVB (Fig. 8). Depletion of tantalum and niobium relative to other incompatible elements in arc lavas has been ascribed to many processes (review in Kelemen *et al.* (2003, p.627)) including: (1) crystal fractionation of Fe-Ti oxides in the crust, (2) fractionation of titanium-rich, hydrous silicates such as phlogopite or hornblende in the mantle or crust, (3) extensive, chromatographic interaction between migrating melt and depleted peridotite, (4) the presence of phases such a rutile or sphene in the mantle wedge, (5) relative immobility of tantalum and niobium relative to REE and other elements in aqueous fluids derived from subducting material, (6) inherited, low Ta/Th and Nb/Th from subducted sediment, and (7) the presence of residual rutile during partial melting of subducted material. Following Kelemen *et al.* (2003) we prefer the hypothesis that fractionation of Nb and Ta from other highly incompatible elements via partial melting of subducting, eclogite facies basalts or sediments with residual rutile to explain the results.

Mygdykit unit basalt compositions vary slightly from plateau to plateau, and Ola Plateau basalts have higher Ni, and lower Sr content compared to rocks from the Arman and Hypotetical plateaus (Figs. 2 and 8). The major elements in the Mygdykit unit of Ola plateau vary slightly, but inconsistently (Fig. 7). The most pronounced co-variation can be seen in graphs of MgO vs SiO₂, CaO, and Na₂O which reflect concurrent fractional crystallization and assimilation processes. Fractional and equilibrium crystallization were simulated using COMAGMAT software (Ariskin and Barmina, 2000) which contains a set of empirically calibrated equations that are used to calculate equilibrium temperatures and phase relations. These equations describe mineral-melt

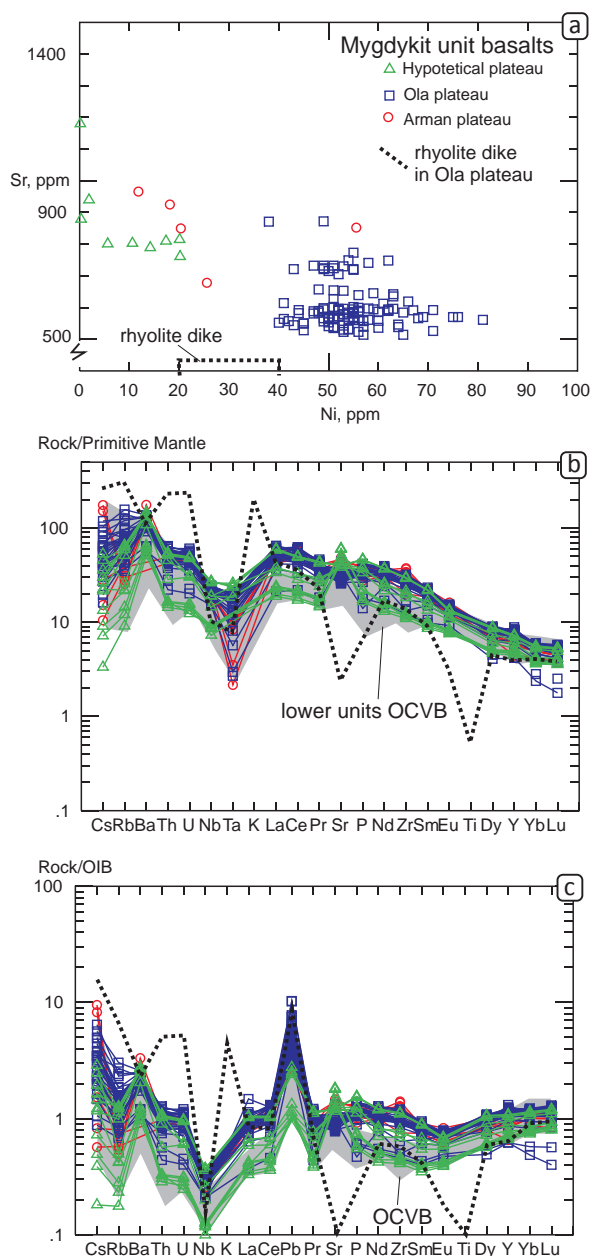


Fig. 8. Trace element diagrams for basalts and basaltic andesites of Mygdykit unit. Figure 8a graph shows compositional variation of basalts from different plateaus. Figure 6b and 6c are spider-diagrams (normalized to primitive mantle and Ocean Island Basalts – OIB, after McDonough and Sun, 1995). Gray field are composition of basalts and andesites from lower units of OCVB. The Mygdykit unit basalts in the lower units of OCVB display notable similar trace element patterns, especially for incompatible trace elements.

equilibria for major- and trace-elements in terms of pressure, temperature, oxygen fugacity and liquid composition. Based on the geothermometers, an algorithm for the simulation of the differentiation of multiply saturated magmas from primitive basalts to dacites has been developed for olivine, plagioclase,

augite, pigeonite (or opx), ilmenite, and magnetite bearing assemblages including the equilibrium mineral proportions and compositions. Simulated liquid lines of descent shows paths that are displaced from the observed major and trace element variation in the Mygdykit unit and therefore indicate that mixing and assimilation processes were involved in the fractionation process (Fig. 7).

In order to estimate the mantle sources for OCVB magmas, radiogenic isotope ratios of Sr, Nd, and Pb were measured in ten samples from the Arman volcanic field (basalts and basaltic andesites of the pre-OCVB Momoltykich Formation, belt andesite of the Narauli and Ulyn formations, rhyolitic ignimbrites of the Ola Formation, and basalts of the Mygdykit Formation). The observed variations in the initial isotopic ratios, $(^{87}\text{Sr}/^{86}\text{Sr})_0 = 0.70444\text{--}0.70332$, $(^{143}\text{Nd}/^{144}\text{Nd})_0 = 0.51286\text{--}0.51257$, ϵNd from +6.5

to +0.8, and $^{208}\text{Pb}/^{204}\text{Pb} = 38.5\text{--}38.04$, suggest that the mantle sources of magmas were rather depleted (similar to MORB) and not significantly different from one another. For instance, the basalts of the Nankala Formation of the OCVB show $(^{87}\text{Sr}/^{86}\text{Sr})_0 = 0.70378\text{--}0.70336$, $(^{143}\text{Nd}/^{144}\text{Nd})_0 = 0.51291\text{--}0.51287$, and ϵNd from +5.3 to +6.1, and the basalts of the pre-belt Momoltykich Formation have almost identical characteristics: $(^{87}\text{Sr}/^{86}\text{Sr})_0 = 0.70378\text{--}0.70336$, $(^{143}\text{Nd}/^{144}\text{Nd})_0 = 0.51291\text{--}0.51287$, and ϵNd from +5.5 to +6.0 (Table 2). The variation of isotopic composition in Mygdykit basalts is reflective of a mixed source from the end-member compositions defined by Zindler and Hart (1986) of PREMA (Prevalent Mantle), BSE (Bulk Silicate Earth), and EM I (Enriched Mantle 1) (Fig. 9). The presence of a relatively depleted MORB-like isotopic component suggests a link between the volcanism

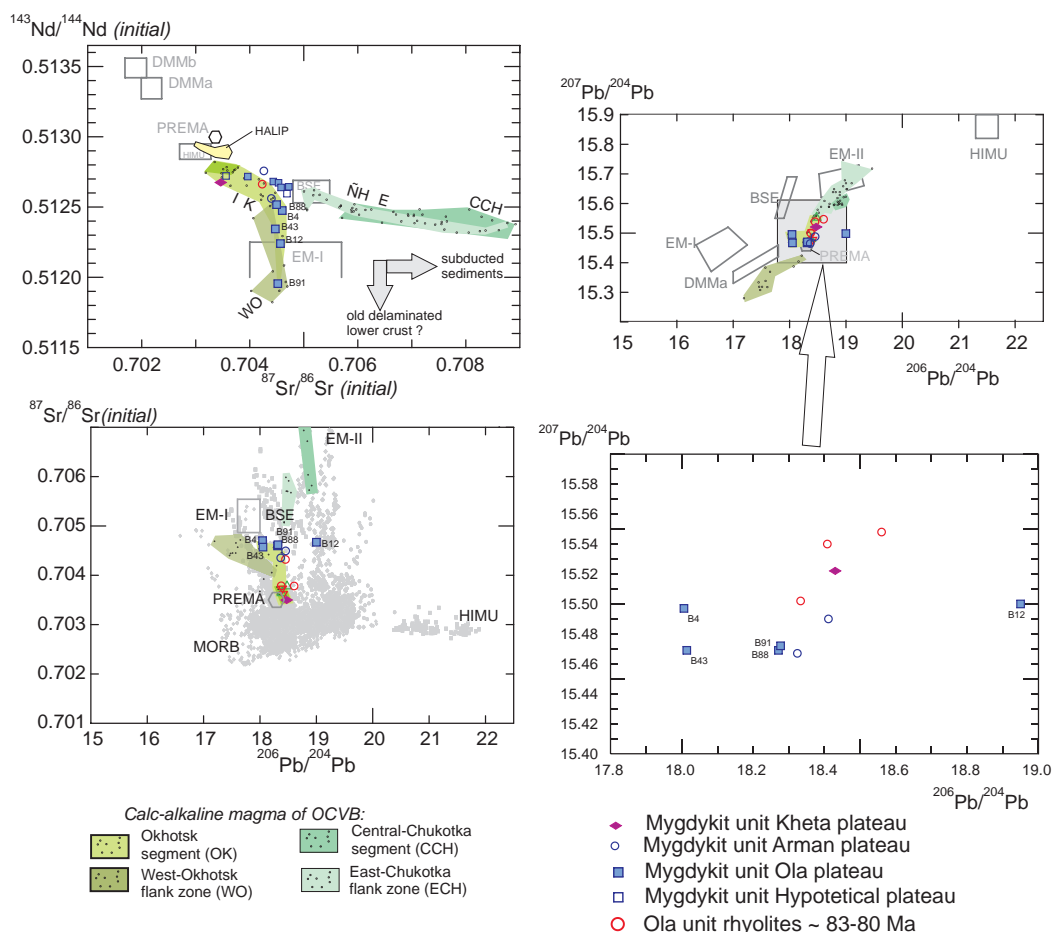


Fig. 9. Isotopic compositions (initial ratios) of the volcanic rocks of the OCVB indicating lateral heterogeneity of the mantle sources of calc-alkaline magmas in various segments and zones of the belt (Akinin and Miller, 2011; Tikhomirov et al., 2008). Symbols with different colors shows basalts of the plateaus of the final stage of OCVB volcanism discussed in this paper (data on basalts from Hypotetical and five samples of Ola plateau are from Leitner, 2010). The mantle end members (DMM, PREMA, BSE, MORB, HIMU, EM-I, EM-II) are after Zindler and Hart (1986).

of the OCVB and subducted oceanic slab. Enriched Sr-Nd isotopic ratios (admixture of EM1 on Fig. 9) may reflect contribution from an old delaminated lower crustal component in the source of magma (Tatsumi and Kogiso, 2003).

Major element compositions in the Ola section vary slightly from the bottom to the top (Fig. 10). SiO₂ increases up section from 49 to 54.5 wt. %, Al₂O₃ from 16 to 17 wt. %, magnesium number (Mg/(Mg+Fe)) from 0.4 to 0.5, K₂O from 1.5 to 2 wt. %. In contrast, TiO₂ decreases up section from 2.2 to 1.4 wt.%, CaO from 8 to 6.5 wt.%, P₂O₅ from 0.8 to 0.6 wt.% decreased up-section (Fig. 10). Trace element variations were not as clear as we found decreasing Ba, but increasing Rb and other incompatible elements with higher positions in the Ola section. In the middle part of the section (flow numbers from B45 to B64) significant shifts in whole rock geochemistry were observed. The most pronounced shifts are strong increases in CaO, Sr, ⁸⁷Sr/⁸⁶Sr isotopic ratio (from 0.7035 to 0.7077 ± 0.0001), and a coincident decrease in SiO₂, Ba, and LOI (Fig.10). The sharp changes in composition between flows 45 to 64 are interpreted to have been caused by an introduction of a CO₂-bearing, Si-rich fluid flux into the magma chamber which led to post-magmatic carbonate alteration and formation of agate and chalcedonies (Akinin et al., 2007).

Microprobe studies of rock-forming minerals (olivine, and plagioclase phenocrysts, as well as clinopyroxene, orthopyroxene, and Fe-Ti oxides in groundmass) were conducted in seventeen representative samples. A total of 310 olivine phenocrysts were studied which revealed a composition variation from Fo 81.8 to Fo 54.2 with most of the olivines having Fo 77-71. We did not find any clear gradational change in composition of olivine across the section. Plagioclase numbers vary from An 88 to An 43 with most of the grains having An 73-60. We found plagioclase with lower An number in older eruptions, whereas plagioclase with higher in anorthite content is located in the middle and upper parts of the section. Clinopyroxene in the groundmass of the lavas displays variation in magnesium number (Mg#=Mg/(Mg+Fe), mol.) within the same samples or the same mineral grains from 0.75 to 0.5, and shows little or no systematic variation with stratigraphic position in the section.

Orthopyroxene microphenocryst compositions measured in four samples have Mg# ranging from 0.73 to 0.51, generally consistent with the variation in Mg# in clinopyroxene. We suggest that the mostly weak variations in whole rock and mineral composition with locations in the section, reflect that fractional crystallization processes were limited. Weak plagioclase fractionation is suggested in magma evolution and is corroborated by the limited changes in whole rock Ca, Sr, and Ba.

DISCUSSION AND CONCLUDING REMARKS

The final stage of basaltic volcanism in Okhotsk segment of Okhotsk-Chukotka volcanic belt occurred during Early Campanian (78-80 Ma) as suggested from ⁴⁰Ar/³⁹Ar and U-Pb SHRIMP dating of the Mygdykit suite of the Ola plateau (northern coast of Okhotsk Sea). Our new ages are close to those obtained from the underlying rhyolite sequences, showing that the hiatus between rhyolite and the overlying Mygdykit basalt unit was less than 1–2 Ma. The small disparity in time between these two units suggests that these plateau basalts are part of the OCVB.

The emplacement of the Mygdykit basalts heralds the final stage of volcanism in the OCVB related to oblique subduction. Simultaneously, the transition coincided with the completion of plume-related tholeiitic volcanism in the HALIP which occurred between ~130 to ~80 Ma (Gottlieb and Miller, 2012), and is possibly linked to the opening of the Canada Basin. The HALIP is a tholeiitic suite that occurs as flood basalt lavas, sills and dykes exposed on the Canadian Arctic Islands, the Chukchi margin, Svalbard and King Charles Land, and Franz Josef Land (e.g. Tegner et al., 2011; Thorarinnsson et al., 2011). Although both final OCVB basalts and HALIP basalts represent disparate geochemical signatures and sources, they might have been caused by a global change in the geodynamics of both Pacific and Arctic regions. This suggests that during the Early Campanian, the direction of Pacific plate motion may have changed dramatically (e.g. Engebretson et al., 1985) from orthogonal subduction along the Russian Pacific margin to a regime of an overall transform margin with local extension zones or slab-windows. Simultaneously,

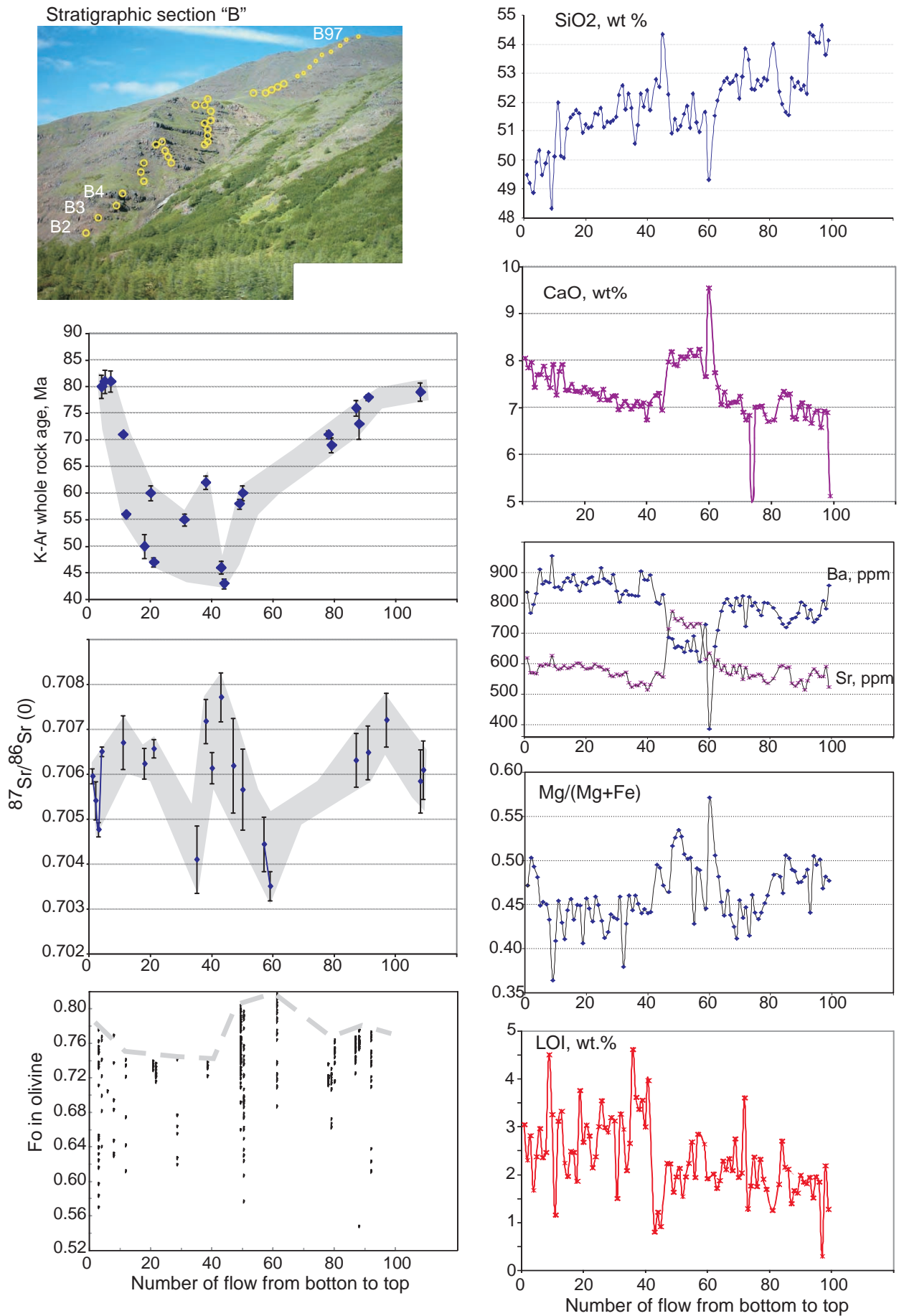


Fig. 10. Variation of composition of basalts and basaltic andesites of Mygdykit unit from Ola plateau from bottom to top of stratigraphic section "B" (Grozovoi Creek).

in the Arctic it was the beginning of extensive initial (pre-breakup) rifting in the Eurasia – Laptev Sea region of Arctic as well as compression events in the Chukchi-Bering region (e.g. Drachev, 2011).

The spiked incompatible trace element patterns of the Mygdykit unit lavas including pronounced Nb-Ta negative anomaly (Fig. 8) are indicative of a component derived from partial melting of eclogite facies subducted material with residual rutile (Kelemen et al., 2003). Volcanic rocks with MgO-rich compositions that are in equilibrium with the mantle wedge are rare in continental arcs and form only a minor component of island arcs, due to density filtering and intracrustal ‘processing’ of ascending magmas (Annen et al., 2006). The maximum values of Mg with a number of about 0.58 (sample B61: whole rock Mg# =0.581, plagioclase An80, olivine Fo81.7) in the Mygdykit unit basalts indicates that they represent a primary mantle-derived melt. On the other hand, all of the samples contain evidence of magma evolution generated during

AFC (assimilation and fractional crystallization) processes from evolved mafic magma. The parent melt probably did not reach the surface, and instead probably stalled in a middle crustal magma chamber or in MASH zones (zone of mixing, assimilation, storage and hybridization; Hildreth and Moorbath, 1988). The most magnesium-rich basalts (e.g. sample B61, B80) can be segregated at pressures of about 7 to 8 kilobars as calculated using appropriate whole rock and plagioclase-melt barometers (Albarede, 1992; Putirka, 2008), and a temperature of 1200 to 1250° C using the plagioclase-melt and olivine-melt thermometers (Putirka, 2008; Beattie, 1993). Basalts with lower contents of MgO (e.g. sample B10, whole rock Mg# =0.41, plagioclase An66, olivine Fo72), according to our calculations using Putirka’s plag-melt equation 25a (2008) were generated at T= 1150-1180° C, and P= 5-6 kb, which corresponds to a depth of about 15 to 18 km where the fractionation took place. Calculated pressures are little lower than those experimentally produced for residual melts

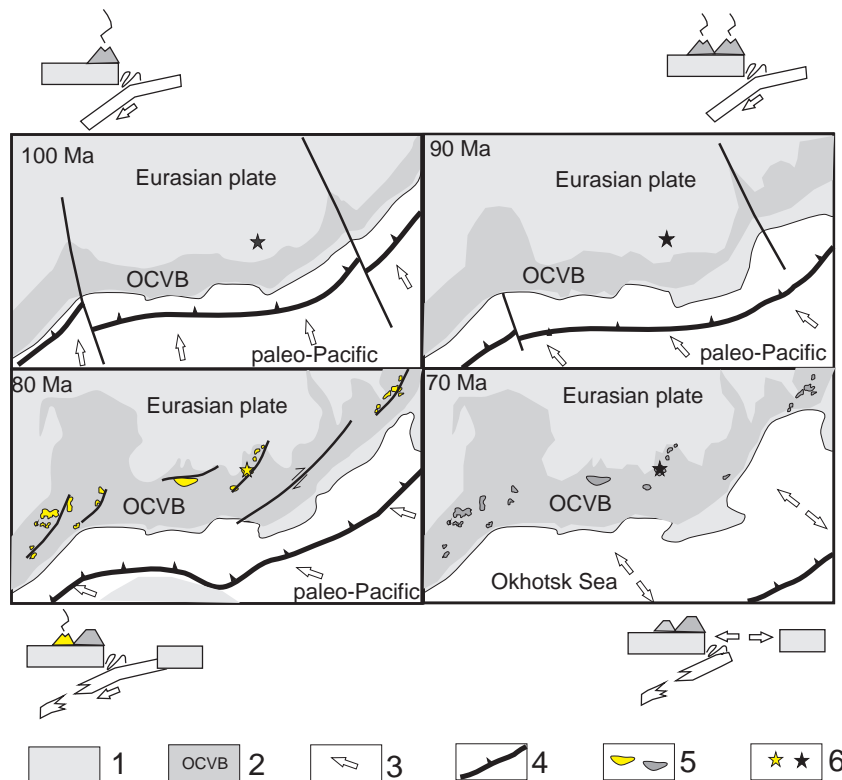


Fig. 11. Paleo-reconstruction schematic showing inferred links between development of late-stage OCVB volcanism (basaltic volcanism of the Mygdykit unit) due to change in geodynamic setting from frontal subduction to a slab-window transform regime along the paleomargin of eastern North eastern Russia. 1 - Eurasian plate, Northeastern Russia; 2 - subduction related Okhotsk-Chukotka continental margin volcanic belt; 3 - plate motion direction; 4 - subduction zone; 5 - active (yellow) and not active (grey) area of Mygdykit unit basaltic volcanism; 6 - position of Ola plateau.

from crystallization of Mount Shasta hydrous basalts in the lower crust (Fig. 7).

Although the Mygdykit unit basalts have subduction-like geochemical features (e.g. Nb-Ta negative anomaly) they display geochemical discrepancies compared to basalt units in the underlying parts of the OCVB. The plateau basalts have higher Ti, Zr, P, and other HFSE as well as more evolved Sr and Nd isotopic ratios compared to the stratigraphically lower basalts which we attribute to a slab-window volcanism or local extension-related volcanism along strike-slip faults. Principal sketch of paleodynamic reconstruction of such environment on four time-slices shown on Fig. 11. We speculate that contrasting tectonic processes in the system “rifted Arctica vs. subducted western Pacifica” at ~80 Ma affected the geodynamic setting in Northern Asia. At this time the subduction setting changed from orthogonal subduction to extension due transform-like continental margin.

Acknowledgments. We greatly appreciated a helpful review by Thomas Moore improving the draft of the manuscript. This study was financially supported by the Russian Foundation for Basic Research, project no 12-05-00874 (PI. Akinin), and CRDF-Far East Branch RAS grant no. RUG1-2994-MA-11 (PIs Akinin and Miller).

Table 2. Geochemistry of Ola plateau volcanic rocks.

Sample No	B1	B2	B3	B4	B7	B11	B18	B21	B28	B31	B35	B38
Longitude	151.313	151.307	151.307	151.307	151.307	151.306	151.306	151.306	151.304	151.304	151.303	151.303
Latitude	60.647	60.648	60.649	60.649	60.649	60.650	60.649	60.650	60.651	60.651	60.650	60.651
SiO ₂	49.49	49.19	48.87	49.92	49.89	51.99	51.62	51.10	51.29	52.25	51.80	52.29
TiO ₂	1.88	2.05	2.06	2.17	2.09	1.97	1.97	1.89	1.86	1.87	1.77	1.69
Al ₂ O ₃	16.95	15.88	15.94	16.15	16.17	16.10	16.31	15.90	15.85	16.30	16.11	15.87
FeOT	9.19	10.31	10.20	10.35	10.00	9.73	9.67	9.48	9.61	9.39	9.31	8.83
MnO	0.15	0.17	0.16	0.16	0.16	0.14	0.13	0.15	0.15	0.12	0.15	0.14
MgO	4.60	5.86	5.57	5.38	4.60	4.55	4.42	4.27	4.22	4.47	4.16	3.90
CaO	8.06	7.85	7.97	7.44	7.89	7.27	7.35	7.34	7.16	6.96	6.97	7.03
Na ₂ O	3.27	3.17	3.25	3.32	3.39	3.54	3.25	3.81	3.83	3.51	3.34	3.52
K ₂ O	1.74	1.40	1.39	1.54	1.54	1.71	1.58	1.22	1.34	1.84	1.90	1.59
P ₂ O ₅	0.58	0.66	0.64	0.73	0.78	0.74	0.74	0.74	0.71	0.73	0.79	0.78
LOI	3.04	2.30	2.81	1.67	2.35	1.15	1.86	3.03	2.88	1.50	2.65	3.36
TOTAL	98.95	98.84	98.86	98.83	98.86	98.89	98.90	98.93	98.90	98.94	98.95	99.00
Mg #	0.471	0.503	0.493	0.481	0.450	0.455	0.449	0.445	0.439	0.459	0.443	0.440
Sc	20	21		22	19	19	21	21	18	20	20	18
Cr	99	137		102	86	84	88	81	77	77	89	89
Ni	28	44		28	27	28	16	15	20	12	12	19
Rb	39	21		30	22	30	22	69	66	39	41	86
Sr	702	638		663	735	728	699	698	725	658	624	677
Y	20	25		27	26	26	27	27	26	27	27	27
Zr	176	225		290	343	370	285	276	385	280	324	441
Nb	8.1	10.8		13.2	12.7	13.4	14.3	13.2	13.7	13.8	16.5	16.2
Cs	1.15	0.81		0.77	0.74	0.91	1.14	2.49	1.90	1.46	1.28	2.18
Ba	723	566	795	708	899	524	730	848	996	764	748	1208
La	27	28		32	30	33	34	35	32	36	40	38
Ce	69	85		80	72	100	88	90	75	99	105	99
Pr	7.3	7.9		9.0	8.6	9.2	9.8	9.9	9.2	9.7	11.1	10.6
Nd	32.2	34.7		39.8	37.1	39.8	42.7	42.7	38.7	41.7	47.3	44.2
Sm	6.6	7.3		8.1	7.6	7.9	8.4	8.4	7.6	8.3	9.1	8.6
Eu	2.1	2.2		2.4	2.2	2.1	2.3	2.3	2.0	2.2	2.2	2.1
Gd	6.8	7.7		8.5	8.1	8.5	8.6	8.8	8.1	8.8	9.8	8.6
Tb	0.81	0.95		1.06	0.98	1.00	1.06	1.07	0.97	1.06	1.10	1.01
Dy	4.3	5.2		5.8	5.2	5.3	5.8	5.8	5.3	5.7	5.9	5.4
Ho	0.8	1.0		1.1	0.9	1.0	1.1	1.1	0.9	1.1	1.1	1.0
Er	2.1	2.7		2.9	2.6	2.7	2.9	2.9	2.6	2.9	3.0	2.7
Tm	0.3	0.3		0.4	0.3	0.3	0.4	0.4	0.3	0.4	0.4	0.3
Yb	1.8	2.3		2.5	2.3	2.3	2.5	2.6	2.3	2.6	2.6	2.3
Lu	0.25	0.34		0.37	0.32	0.31	0.37	0.37	0.31	0.38	0.38	0.32
Hf	3.7	4.6		5.3	4.7	5.2	5.8	5.5	5.3	5.7	6.5	6.0
Ta	0.47	0.61		0.73	0.77	0.65	0.78	0.73	0.65	0.77	0.73	0.71
Pb	16.0	17.2		20.3	15.1	32.7	32.9	20.3	24.8	24.2	18.2	18.8
Th	4.4	3.4		3.7	3.2	3.8	4.4	4.4	3.5	4.1	4.4	4.0
U	1.1	0.9		0.9	0.8	1.0	1.1	1.0	0.9	1.0	1.1	1.0
K-Ar age, Ma				80	81	71	50	47	0	55	0	62
1σ				2.2	2.0	0.5	2.2	0.9		1.1		1.3
⁸⁷ Sr/ ⁸⁶ Sr	0.70619	0.70556	0.70497	0.70484		0.70479	0.70639	0.70699			0.7044	0.70775
2σ	0.00017	0.00042	0.00016	0.000010		0.000001	0.000345	0.0002			0.00075	0.00049
(⁸⁷ Sr/ ⁸⁶ Sr) _i	0.70597	0.70542	0.70478	0.704648		0.704614	0.70624	0.70658			0.70411	0.70719
¹⁴³ Nd/ ¹⁴⁴ Nd				0.512539		0.512293						
2σ				0.00001		0.00001						
(¹⁴³ Nd/ ¹⁴⁴ Nd) _i				0.512476		0.512232						
ε _{Nd}				-1.2		-6.0						
T _{Nd} (DM)				884		1228						
²⁰⁶ Pb/ ²⁰⁴ Pb				18.01		18.95						
²⁰⁷ Pb/ ²⁰⁴ Pb				15.50		15.50						
²⁰⁸ Pb/ ²⁰⁴ Pb				37.85		37.93						

Sample numbers with * indicate late dikes, (⁸⁷Sr/⁸⁶Sr)_i and (¹⁴³Nd/¹⁴⁴Nd)_i are calculated initial ratios.

Sample No	B40	B43	B47	B50	B57	B59	B78	B87	B91	B97	BD61*	KA524-7*
Longitude	151.303	151.303	151.301	151.301	151.301	151.301	151.300	151.299	151.299	151.324	151.301	151.261
Latitude	60.651	60.651	60.652	60.652	60.653	60.653	60.655	60.656	60.656	60.661	60.653	60.661
SiO ₂	52.42	52.80	52.28	51.03	50.96	51.66	52.83	52.83	52.57	54.64	49.42	75.34
TiO ₂	1.73	1.75	1.64	1.53	1.63	1.77	1.77	1.70	1.73	1.64	1.27	0.11
Al ₂ O ₃	15.91	16.36	17.15	16.89	17.28	16.83	16.15	16.38	16.28	16.70	17.42	13.93
FeOT	8.98	9.12	8.26	8.74	8.42	8.85	8.97	8.94	8.93	8.38	8.95	0.86
MNO	0.13	0.15	0.13	0.14	0.15	0.15	0.14	0.13	0.15	0.14	0.15	0.01
MGO	3.96	5.01	4.02	5.63	4.52	3.99	4.15	4.81	4.65	4.14	6.96	0.08
CAO	6.74	7.26	7.98	7.89	8.25	7.67	6.86	6.80	6.77	6.93	9.66	0.14
NA ₂ O	3.34	3.51	3.40	3.12	3.38	3.44	3.43	3.47	3.41	3.56	2.85	1.62
K ₂ O	1.97	1.51	1.28	1.45	0.97	1.35	1.95	1.91	1.99	1.98	1.03	6.03
P ₂ O ₅	0.80	0.68	0.68	0.66	0.64	0.68	0.83	0.63	0.67	0.66	0.28	0.00
LOI	2.99	0.80	2.23	1.95	2.84	2.63	1.90	1.39	1.84	0.29	1.00	1.79
TOTAL	98.97	98.95	99.05	99.03	99.04	99.02	98.98	98.99	98.99	99.06	98.99	100.00
Mg #	0.440	0.495	0.464	0.534	0.489	0.446	0.452	0.490	0.481	0.468	0.581	0.142
Sc	21	21	23	19	20	21	18	21	15	16	26	1
Cr	91	111	96	100	79	75	91	102	90	80	142	1
Ni	12	30	9	21	16	19	21	33	28	12	38	36
Rb	50	75	40	23	35	56	44	42	37	43	21	190
Sr	625	677	875	862	886	752	641	640	524	655	809	51
Y	28	28	26	23	24	27	27	26	24	27	22	21
Zr	336	293	276	244	250	290	333	287	266	410	127	163
Nb	16.9	13.7	12.4	11.5	11.8	14.0	17.4	14.2	13.6	14.8	3.7	10.0
Cs	1.71	1.32	1.34	0.63	0.85	1.48	1.35	1.19	1.03	0.90	0.57	
Ba	712	751	572	268	227	1636	561	1549	244	329	282	707
La	42	37	36	33	32	35	41	33	31	38	24	29
Ce	97	83	84	83	79	91	100	86	76	89	56	62
Pr	11.8	10.2	10.4	9.6	9.2	10.1	11.4	9.5	8.6	10.7	6.9	6.0
Nd	49.3	43.7	44.7	41.7	39.8	43.5	48.2	40.2	37.0	45.3	30.2	21.9
Sm	9.5	8.5	8.6	8.1	7.7	8.5	9.2	7.9	7.1	8.7	6.1	3.9
Eu	2.3	2.2	2.4	2.2	2.2	2.2	2.2	2.0	1.8	2.1	1.8	0.5
Gd	9.4	8.7	8.7	7.9	7.8	8.6	9.2	8.1	7.3	8.7	6.4	4.0
Tb	1.14	1.09	1.04	0.94	0.94	1.06	1.12	1.01	0.91	1.07	0.77	0.52
Dy	6.0	5.9	5.5	5.2	5.2	5.9	6.1	5.7	5.2	5.9	4.3	3.1
Ho	1.1	1.1	1.0	0.9	0.9	1.1	1.1	1.0	1.0	1.1	0.8	0.6
Er	3.0	3.0	2.8	2.6	2.6	3.0	3.0	2.9	2.7	3.0	2.3	1.8
Tm	0.4	0.4	0.4	0.3	0.3	0.4	0.4	0.4	0.3	0.4	0.3	0.3
Yb	2.6	2.6	2.5	2.3	2.3	2.6	2.6	2.5	2.3	2.6	2.0	1.9
Lu	0.39	0.38	0.36	0.32	0.33	0.38	0.37	0.37	0.33	0.36	0.28	0.27
Hf	6.8	6.0	5.6	5.1	5.1	6.0	6.7	5.9	5.3	6.4	2.6	4.3
Ta	0.74	0.72	0.67	0.44	0.46	0.60	0.73	0.61	0.54	0.59	0.21	0.30
Pb	16.4	17.2	12.2	13.6	13.5	17.9	15.0	11.7	11.4	23.9	11.1	25.6
Th	4.8	4.8	3.8	3.4	3.3	5.1	4.5	4.5	3.8	5.0	3.0	19.0
U	1.2	1.1	0.9	0.9	0.8	1.1	1.1	1.1	1.0	1.2	0.7	5.0
K-Ar age, Ma	0	46	0	60	0	0	71	76	78	0	61	
1σ		1.2		1.4			0.7	1.4	0.5		1.2	
⁸⁷ Sr/ ⁸⁶ Sr	0.7065	0.70499	0.7064	0.7058	0.7046	0.70382		0.70484	0.70487	0.7075	0.7056	
2σ	0.00035	0.00001	0.00105	0.0009	0.0006	0.00033		0.000010	0.00002	0.0006	0.00065	
(⁸⁷ Sr/ ⁸⁶ Sr) _i	0.70614	0.704518	0.70620	0.70567	0.70445	0.70352		0.704541	0.70456	0.70722	0.70549	
¹⁴³ Nd/ ¹⁴⁴ Nd		0.51240						0.512519	0.51201			
2σ		0.00001						0.00001	0.00001			
(¹⁴³ Nd/ ¹⁴⁴ Nd) _i		0.512344						0.512519	0.51195			
ε _{Nd}		-3.8						-0.4	-11.4			
T _{Nd} (DM)		1034						409	1575			
²⁰⁶ Pb/ ²⁰⁴ Pb		18.01						18.27	18.28			
²⁰⁷ Pb/ ²⁰⁴ Pb		15.47						15.47	15.47			
²⁰⁸ Pb/ ²⁰⁴ Pb		37.93						38.06	38.07			

REFERENCES

- Akinin V.V., Miller E.L., Wooden J., 2009. Petrology and Geochronology of Crustal Xenoliths from the Bering Strait Region: Linking Deep and Shallow Processes in Extending Continental Crust. Geological Society of America Special Paper 456, 39–68.
- Akinin, V.V. and E. L. Miller, 2011. The evolution of the calc-alkalic magmas of the Okhotsk – Chukotka volcanic belt. *Petrology*. 19, № 3, 237-277.
- Akinin V.V., Alshevsky A.V., Parfenov M.I., Leonova V.V., 2007. Age and evolution of Ola plateau basaltic magma, northern Priokhotie. In: All Russian conference dedicated to academician K.V.Simakov. Abstract volume. Magadan, NEISRI FEB RAS. 5 (in Russian)
- Alshevsky A.V., 1997. About upper age limit of continental margin OCVB. In: Geological formation, magmatism, and ore deposits of North-Eastern Asia, Abstracts of Mineralogical conference, Magadan, NEISRI FEB RAS. 43-45 (in Russian)
- Albarède, F., 1992. How deep do common basaltic magmas form and differentiate? *Journal of Geophysical Research*, 97, 10997-11009.
- Anderson, D.L., 2001. Top-down tectonics? *Science*, 293, 2016–2018.
- Annen, C., J. D. Blundy, R. S. J. Sparcs, 2006. The Genesis of Intermediate and Silicic Magmas in Deep Crustal Hot Zones, *Journal of Petrology*, 47(3), 505-539.
- Anorov P.N., Bychkov Yu.M., Karavaeva N.I., Mikhailov V.P., Yudina G.M., 1999. Geological map 1:200 000 scale legend for Magadan series, Russian Federation (2th edition), Magadan, Ministry of natural resources of Russian Federation, 110 p. (in Russian)
- Ariskin A.A., Barmina G.S., 2000. Modelling phase equilibria at crystallization of basalt magmas, Moscow, Nauka, MAIK «Nauka/ Interperiodica», 363p. (in Russian)
- Beattie P., 1993. Olivine-melt and orthopyroxene-melt equilibria: Contributions to Mineralogy and Petrology, 115, 103-11.
- Belyi, V.F., 1977. Stratigraphy and Structure of the Okhotsk–Chukotka Volcanogenic Belt. Moscow: Nauka, 190p. (in Russian)
- Bely V.F., Belaya, B.V., 1998. Late stage of evolution of Okhotsk-Chukotka volcanogenic belt (upper part of Enmyvaam River). Magadan, NESRI FEB RAS, 108p. (in Russian).
- Belyi, V.F., 2008. Problems of Geological and Isotopic Age of the Okhotsk–Chukotsk Volcanogenic Belt (OCVB). *Stratigr. Geol. Correlation*, 16 (6), 639–649.
- Bercovici, D., 2003. The generation of plate tectonics from mantle convection. *Earth Planet. Sci. Lett.* 205, 107–121.
- Condie K.C., 2003. Incompatible element ratios in oceanic basalts and komatiites: Tracking deep mantle sources and continental growth rates with time: *Geochemistry, Geophysics, Geosystems*. 4(1), doi:10.1029/2002GC000333.
- Drachev S.S., 2011. Tectonic setting, structure and petroleum geology of the Siberian Arctic offshore sedimentary basins. In: Spencer A.M., Embry, A. F., Gautier, D. L., Stoupakova, A. V. & Sorensen, K. (Eds.) *Arctic Petroleum Geology, Memoirs*, 35. London: The Geological Society of London, 369–394 (DOI: 10.1144/M35.25).
- Engebretson, D.C., Cox, A., Gordon, R.G., 1985. Relative motions between oceanic and continental plates in the Pacific Basin. *Geological Society of America Special Paper*. Boulder, Colorado, 59 p.
- Filatova, N.I., 1988. Peri-oceanic Volcanogenic Belts. Moscow, Nedra, 264 p. (in Russian)
- Gottlieb, E., and Miller, E., 2012. Cretaceous Magmatism in the Arctic: Slab versus Plume? Or Slab and Plume Together?, ICAM-VI. Conference abstracts. Geophysical Institute Report UAG-R-335, Compilers: D.B.Stone, J.G.Clough, D.K.Thurston, University of Alaska, Fairbanks, Alaska, 63-64.
- Gorodinsky, M.E. (Ed.), 1980. Geological map of North East USSR, 9 sheets, 1:1,500,000 scale. *Minist. Geol. SSSR, Leningrad*, (in Russian).
- Grove, T. L., Elkins-Tanton, L. T., Parman, S. W., Chatterjee, N., Muntener, O., Gaetani, G. A., 2003. Fractional crystallisation and mantle-melting controls on calc-alkaline differentiation trends. *Contributions to Mineralogy and Petrology*, 145, 515–533.
- Hildreth, W., and Moorbath, S., 1988. Crustal

- contribution to arc magmatism in the Andes of Central Chile. *Contributions to Mineralogy and Petrology* 98, 455–489.
- Hourigan J.K. and Akinin V.V., 2004. Tectonic and chronostratigraphic implications of new $^{40}\text{Ar}/^{39}\text{Ar}$ geochronology and geochemistry of the Arman and Maltan-Ola volcanic fields, Okhotsk-Chukotka volcanic belt, northeastern Russia, *Geol. Soc. Am. Bull.*, 116 (5-6). 637-654.
- Ispolatov, V.O., Tikhomirov, P.L., Heizler, M., Cherepanova, I.Yu., 2004. New $^{40}\text{Ar}/^{39}\text{Ar}$ Ages of Cretaceous Continental Volcanics from Central Chukotka: Implications for Initiation and Duration of Volcanism within the Northern Part of the Okhotsk Chukotka Volcanic Belt (Northeastern Eurasia). *J. Geol.*, 112, 369-377.
- Kawamoto, T., 1996. Experimental constraints on differentiation and H₂O abundance of calc-alkaline magmas. *Earth and Planetary Science Letters* 144, 577–589.
- Kelemen, P.B., Hanghoj, K., and Greene, A.R., 2003. One view of the geochemistry of subduction-related magmatic arcs, with an emphasis on primitive andesite and lower crust. in *The Crust*, Rudnick R.L., Ed., *Treatise on Geochemistry*, Amsterdam: Elsevier. 3, 593–569.
- Kelley S.R., Spicer R.A., Herman A.B., 1999. New $^{40}\text{Ar}/^{39}\text{Ar}$ dates for Cretaceous Chauna Group tephra, north-eastern Russia, and their implications for the geologic history and floral evolution of the North Pacific region, *Cretaceous Research*, 20, 97-106.
- King, S.D., Lowman, J.P., Gable, C.W., 2002. Episodic tectonic plate reorganizations driven by mantle convection. *Earth Planet. Sci. Lett.*, 203, 83–91.
- Kotlyar, I.N., and Rusakova, T.B., 2004. Cretaceous Magmatism and Ore Potential of the Okhotsk–Chukotka Area: Geological–Geochronological Correlation. Magadan: SVKNII DVO RAN, 152 p. (in Russian).
- Koren', T.N. and Kotlyar, G.V., (Eds.), 2009. Resolution of the 3rd Interdisciplinary Regional Stratigraphic Conference on the Precambrian, Paleozoic, and Mesozoic of Northeastern Russia. St. Petersburg: VSEGEI, 268 p. (in Russian)
- Lanphere, M.A., and Dalrymple, G.B., 2000. First-principles calibration of ^{38}Ar tracers: Implications for the ages of $^{40}\text{Ar}/^{39}\text{Ar}$ fluence monitors, U.S. Geological Survey Professional Paper 1621, 10 p.
- Layer, P.W., 2000. Argon-40/argon-39 age of the El'gygytgyn impact event, Chukotka, Russia, *Meteoritics and Planetary Science*, 35, 591-599.
- Layer, P.W., Hall, C.M. and York, D., 1987. The derivation of $^{40}\text{Ar}/^{39}\text{Ar}$ age spectra of single grains of hornblende and biotite by laser step heating. *Geophys. Res. Lett.*, 14, 757-760.
- LeBas, M.J., LeMaitre, R.W., Streckeisen, A., and Zanettin, B., 1986. A chemical classification of volcanic rocks based on the total alkali silica diagram. *J. Pet.* 27, 745-750.
- Leitner J., 2010. Geochemical and petrological studies of the Ola- and Hypotetica-Plateau basalts in the Okhotsk-Chukotka Volcanic Belt, NE Russia. Unpublished Master Thesis, University of Vienna. 84p.
- Matthews, K. J., M. Seton, and R. D. Müller, 2012. A global-scale plate reorganization event at 105–100Ma, *Earth and Planetary Science Letters*, 355-356, 283-298.
- McDonough W.F., Sun S., 1995. The composition of the Earth, *Chemical Geology*, 120, 223-253.
- McDougall, I. and Harrison, T.M., 1999. *Geochronology and ThermoChronology by the $^{40}\text{Ar}/^{39}\text{Ar}$ method*, 2nd ed. Oxford University Press, New York, 269p.
- Newberry R., Layer, P., Gans, P., Goncharov V.I., Goryachev N.A., Voroshin S.V., 2000. Preliminary geochronology analysis of Mesozoic magmatism, tectonics, and mineralization in North-East Russia according to $^{40}\text{Ar}/^{39}\text{Ar}$ dating and trace element data on igneous and ore-bearing rocks, Gold mineralization and granitoid magmatism of North Pacific. Vol 1. Proceedings of the All-Russian Meeting. Magadan: NEISRI. FEB RAS, 158-205 (in Russian).
- Parfenov, L.M., 1984. Continental Margins and Island Arcs of Northeastern Asian Mesozooids. Novosibirsk: Nauka, 192 p. (in Russian)

- Pearce, J.A., Cann, J.R., 1973. Tectonic setting of basic volcanic rocks determined using trace element analysis. *Earth Planet. Sci. Letters*, 19, 290-300.
- Peccerillo, A. and Taylor, S.R., 1976. Geochemistry of Eocene calc-alkaline volcanic rocks from the Kastamonu area, Northern Turkey. *Contrib. Mineral. Petrol.* 58, 63-81.
- Polin, V.F. and Moll-Stalcup, E.J., 1999. Petrological–Geochemical Criteria of Tectonic Conditions of the Formation of the Chukotka Chain of the Okhotsk–Chukotka Volcanogenic Belt. *Pacific Geology*, 18 (4), 29–47.
- Putirka K.D., 2008. Thermometers and barometers for volcanic systems. *Reviews in mineralogy and geochemistry*, 69, 61-120.
- Sakhno, V.G., Polin, V.F., Akinin, V.V., Sergeev, S.A., Alenicheva, A.A., Tikhomirov, P.L., Moll-Stalcup, E.J., 2010. The diachronous formation of the Enmyvaam and Amguema–Kanchalan volcanic fields in the Okhotsk–Chukotka Volcanic Belt (NE Russia): evidence from isotopic data. *Doklady Earth Sciences* 434 (1), 1172–1178.
- Samson S. D., and Alexander E. C., 1987., Calibration of the interlaboratory $^{40}\text{Ar}/^{39}\text{Ar}$ dating standard, MMhb1. *Chemical Geology*, 66, 27-34.
- Seton, M., Müller, R. D., Zahirovic, S., Gaina, C., Torsvik, T., Shephard, G., Talsma, A., Gurnis, M., Turner, M., Maus, S., Chandler, M., 2012. Global continental and ocean basin reconstructions since 200 Ma. *Earth-Science Reviews*, 113(3-4), 212-270.
- Steiger, R.H. and Jaeger, E., 1977. Subcommittee on geochronology: Convention on the use of decay constants in geo and cosmochronology. *Earth and Planet Science Letters*, 36, 359-362.
- Stone, D.B., Layer, P.W., and Raikevich, M.I., 2009. Age and Paleomagnetism of the Okhotsk–Chukotka Volcanic Belt (OCVB) near Lake El'gygytgyn, Chukotka, Russia, *Stephan Mueller Spec. Publ. Ser.*, 4, 243–260.
- Struzhkov, S.F. and Konstantinov, M.M., 2005. *Metallogeniya zolota i serebrya Okhotsko-Chukotskogo vulkanogenogo poyasa (Gold and Silver Metallogeny of the Okhotsk–Chukotka Volcanogenic Belt)*. Moscow: Nauchnyi Mir, 320 p. (in Russian).
- Tatsumi, Y. and Kogiso, T., 2003. The subduction factory: Its role in the evolution of the Earth's crust and mantle. In: Larter, R.D., and Leat, P.T., eds., *Intra-oceanic subduction systems: tectonic and magmatic processes*. London, Geological Society Special Publication 219, 55–80.
- Tegner, C., Storey, M., Holm, P.M., Thorarinsson, S.B., Zhao, X., Lo, C.-H., and Knudsen, M.F., 2011. Magmatism and Eureka deformation in the High-Arctic Large Igneous Province: $^{40}\text{Ar}/^{39}\text{Ar}$ age of Kap Washington Group volcanics, North Greenland. *Earth Planet. Sci. Lett.* 303, 203-214.
- Tikhomirov P.L., Kalinina E.A., Kobayashi K., Nakamura E., 2008. Late Mesozoic silicic magmatism of the North Chukotka area (NE Russia): Age, magma sources, and geodynamic implications. *Lithos*, 105. 329-346.
- Tikhomirov, P. L., E. A. Kalinina, T. Moriguti, A. Makishima, K. Kobayashi, I. Y. Cherepanova, and E. Nakamura, 2012. The Cretaceous Okhotsk–Chukotka Volcanic Belt (NE Russia): Geology, geochronology, magma output rates, and implications on the genesis of silicic LIPs. *Journal of Volcanology and Geothermal Research*, 221-222, 14-32.
- Thorarinsson, S.B., Holm, P.M., Duprat, H., and Tegner, C., 2011. Silicic magmatism associated with Late Cretaceous rifting in the Arctic Basin – petrogenesis of the Kap Kane sequence, the Kap Washington Group volcanics, North Greenland. *Lithos*, 125 (1-2), 65-85.
- Umitbaev, R.B., 1986. *Okhotsko-Chaunskaya metallogenicheskaya provintsiya (Okhotsk–Chauna Metallogenic Province)*. Moscow: Nauka, (in Russian)
- Ustiev, E.K., 1959. *Okhotsk Tectonomagmatic Belt and Some Related Problems*. *Otechestvennaya geologiya*, 3, 3–26.(in Russian)
- York, D., Hall, C.M., Yanase, Y., Hanes, J.A., and Kenyon, W.J., 1981. $^{40}\text{Ar}/^{39}\text{Ar}$ dating of terrestrial minerals with a continuous laser. *Geophys. Res. Lett.*, 8, 1136-1138.
- Wood, D. A., 1980. The application of a Th-Hf-Ta diagram to problems of tectonomagmatic classification and to establishing the nature of crustal contamination of basaltic lavas of the British Tertiary volcanic province. *Earth and*

Planetary Science Letters, 50 (1), 11-30.

Zhulanova, I.L., Rusakova, T.B., and Kotlyar, I.N.,
2007. Geochronology and Geochronometry of
Endogenous Events in the Mesozoic History
of Northeast Asia. Moscow: Nauka, 358 p. (in
Russian)

Zindler A. and Hart S., 1986. Chemical Geodynamics,
Annual Review of Earth and Planetary Sciences.
14. 493-571.